gases

MDPI

Review

A Review of Fugitive Methane Emissions Detection Technologies for LNG Operations

Nicholas N. A. Ling [1], Mauricio Di Lorenzo [2,3], Luke McElroy [1,3], Kwanghee Jeong [4], Eric F. May [1,3], Michael L. Johns [1,3], Craig E. Buckley [2,3] and Bruce W. E. Norris [1,3,*]

[1] Department of Chemical Engineering, the University of Western Australia, Crawley, WA 6009, Australia
[2] Department of Physics and Astronomy, Curtin University, Kent St., Bentley, WA 6102, Australia
[3] Future Energy Exports Cooperative Research Centre, Crawley, 6009 WA, Australia
[4] Department of Mechanical System Engineering, Jeonbuk National University, 567 Baekje-Daero, Deokjin-Gu, 54896 Jeonju, Jeollabuk-Do, Republic of Korea
* Correspondence: bruce.norris@uwa.edu.au

Abstract

Liquefied natural gas (LNG) is increasingly central to global energy strategy, positioned as a lower-emission transition fuel. That positioning assumes fugitive methane emissions across the LNG supply chain are well-characterised, yet direct measurement campaigns at LNG facilities have found operator-reported inventories capturing only 59–83% of actual emissions—a gap that legacy emission factors derived from upstream U.S. oil and gas facilities are poorly equipped to resolve. As measurement-based accountability replaces estimation factors in voluntary frameworks and emerging regulation, the question is which technologies are fit for purpose. This review provides a comprehensive, cross-scale assessment of methane-sensing technologies—from component-level leak detection through to satellite surveillance—evaluated against the physical and operational realities of LNG facilities. Trade-offs in sensitivity, spatial and temporal resolution, environmental dependence, and regulatory readiness are assessed to determine where each performs reliably and where it falls short. While technology is mature at the component level, validation data specific to LNG environments is scarce across all scales, and no single platform provides a complete solution. The most consequential gaps are methodological: the absence of standardised validation protocols, inadequate regulatory harmonisation, and a persistent lag between instrument capability and accepted practice. Six recommendations are proposed: standardised field validation protocols, hybrid monitoring frameworks, regulatory pathways that accommodate emerging technologies, measurement infrastructure in LNG-intensive regions, data transparency with top-down/bottom-up reconciliation, and improved monitoring coverage for intermittent and difficult-to-access fugitive emissions. Together, these define a roadmap for closing the gap between current practice and the accountability that credible LNG reporting demands.

Keywords: fugitive methane emissions; liquefied natural gas; emissions quantification; gas sensing; remote sensing

Academic Editor: Lionel Ganippa

Received: 27 August 2026
Revised: 20 October 2026
Accepted: 26 October 2026
Published: 1 November 2026

Copyright: © 2026 by the authors. Licensee MDPI, Basel, Switzerland. This article is an open access article distributed under the terms and conditions of the Creative Commons Attribution (CC BY) license.

1. Introduction

Methane, the major component of natural gas, is considered one of the most important greenhouse gases (GHGs). Its global warming potential (GWP) relative to carbon dioxide, one of the most abundant atmospheric GHGs, is 120 gCO_{2eq}/gCH_4 [1]. Because its atmospheric lifetime is only ~12 years, methane's GWP declines over time, giving a 20-year GWP (GWP20) of ~80 and a 100-year GWP (GWP100) of 28 (this means that the average radiative forcing of a methane emission over 100 years after the emission is 28 times that of an equivalent mass of CO_2, including climate carbon feedback effects) [1,2]. Atmospheric methane has risen since the Industrial Revolution, reaching 1946 ppb in November 2025, 2.7 times its 1750 level [3]. This increase, mainly anthropogenic, accounts for an estimated 30% of the additional temperature rise in the lower atmosphere [4]. Methane is now a central focus of climate policy worldwide [5]. The energy sector—oil, natural gas, coal, and bioenergy—accounts for more than 35% of anthropogenic emissions, with oil and gas alone contributing around 80 Mt CH_4 in 2024 [4]. This includes fugitive emissions (unintentional releases of gas from pressurised systems such as valves, flanges, compressors, and seals) as well as vented and incomplete flaring emissions across the hydrocarbon supply chain.

At LNG facilities, potential fugitive methane sources are distributed across gas processing, liquefaction or regasification, boil-off gas handling, storage, and transfer systems. In addition to the components identified above, leaks can occur through isolation valves connected to open-ended lines and at loading-arm connections. Measurements covering an entire process area may capture both equipment leaks and emissions from venting or incomplete combustion. These contributions therefore need to be distinguished when assessing the relative importance of fugitive methane sources.

LNG-specific measurements provide examples of the proportion of components found leaking and their contributions to emissions. At one LNG terminal in China, 252 of 3243 inspected components (7.77%) were identified as leaking using a screening concentration threshold of 100 ppm [6]. Based on the estimated emissions reported for each component category at that terminal, flanges contributed approximately 40.9% of the total fugitive emissions from the surveyed components, valves 29.5%, open-ended lines 17.6%, and connectors 12.0%. At another regasification facility, a leak associated with the jetty loading arms accounted for approximately 17% of the total site methane emissions reported during the measurement campaign [7]. This 17% represents a share of total measured site methane emissions, including sources other than equipment leaks. These findings demonstrate the importance of individual sources but do not establish representative contributions across LNG facilities.

Leak frequency and duration are less clearly characterised by these surveys. The proportion of components found leaking during an inspection does not indicate how frequently new leaks develop or how long existing leaks persist. Establishing these characteristics requires repeated observations or continuous monitoring, supported by operating and repair records. Because cumulative emissions depend on both emission rate and duration, short measurement campaigns also provide an incomplete basis for estimating annual source contributions. These limitations support combining component inspections with monitoring that captures changes in emissions over time.

These uncertainties also complicate emission estimates based on generic engineering emission factors. Such factors have historically been derived from large U.S. datasets collected at multi-well sites and compressor stations. Studies of thousands of measurements across major U.S. production regions show that leak size distributions for compressors, flanges, and valves span at least two orders of magnitude, so a small number of large leaks dominate total emissions [8]. How strongly these distributions depend on

geographical location (e.g., facilities in less or more regulated countries) and on position in the supply chain (upstream, midstream, downstream) adds further uncertainty.

Large datasets exist for multi-well and compressor-station environments, but data specific to LNG plants are scarce. Only one comprehensive campaign has focused on LNG facilities: Innocenti, et al. [7] from the UK National Physical Laboratory (NPL) employed a Differential Absorption Laser-Light Detection and Ranging (DIAL) system to quantify methane emissions from two regasification and three liquefaction facilities across different regions. Average methane losses were 0.018% of throughput at regasification facilities and 0.070% at liquefaction facilities, while operator-reported inventories captured only 59–83% of the measured emissions—a direct demonstration of how measurement improves the accuracy of emission factors and facility-level inventories. Airborne surveys at four Australian LNG liquefaction facilities evaluated mass-balance and CO_2 tracer correlation methods for estimating site-level CH_4 emissions [9]. The multi-height tracer approach produced estimates consistent with mass balance and showed potential for lower uncertainty, provided that measurements adequately covered the plume and CO_2 emission rates were sufficiently well characterised.

Regulatory frameworks vary globally, with many jurisdictions still relying on legacy estimation protocols. The Australian National Greenhouse and Energy Reporting (Measurement) Determination (NGER(M)D), which adopts U.S. standards, has no approved method for direct measurement of area or point-source fugitive emissions. While operators may seek approval to implement emerging technologies, the default methods, such as Method 3 [10], based on the U.S. EPA's Method 21 [11], rely on indirect leak detection via concentration thresholds and engineering correlations, rather than direct quantification. Bagging techniques (vacuum, blow-through, and high-flow sampling) can measure leak rates directly but have been underutilised for practical reasons [11]. Optical gas imaging (OGI) cameras, however, can both detect and quantify methane emissions, with detection limits of 60 g CH_4/h [10,12,13]. Recent studies and regulatory developments, including the U.S. EPA's draft protocol for OGI-based quantification [14], support the integration of such technologies into Leak Detection and Repair (LDAR) programmes [15]. Equivalence frameworks are emerging to test whether alternative methods deliver at least the same mitigation outcomes as traditional approaches. Fox, et al. [15] proposed a five-stage framework combining controlled testing, simulation modelling, and field trials to systematically evaluate new LDAR technologies against conventional methods. Using the FEAST simulation tool, Kemp and Ravikumar [16] demonstrated that new technologies such as drones, planes, and satellites can achieve equivalent emissions reductions to OGI-based LDAR at lower cost by optimising survey frequency. However, technology equivalence varied significantly across basins, cautioning against blanket regulatory approval of new methods across regions.

Growing empirical evidence [4,8,17,18] suggests that current inventory (calculation) methods may in some cases underestimate actual emissions. Leak data from natural gas production facilities indicate that most emissions originate from high-rate leaks (>2.5 kg CH_4/h (70 kg $CO_{2\text{-e/h}}$)), which are often missed by infrequent or narrowly focused surveys [8]. The MONITOR ARPA-E project [19], for example, targets emissions at a sensitivity threshold of ~0.11 kg CH_4/h (3.2 kg $CO_{2\text{-e/h}}$). This threshold is approximately 1.8 times the 0.06 kg CH_4/h detection sensitivity currently prescribed by regulation and achievable with OGI [10]. Minimum detection limits alone, however, are insufficient to evaluate a detection method. Emission distribution, instrument type (ground-based vs. aerial), ease of deployment, and operator proficiency all shape real-world performance. Because large, infrequent events account for a substantial share of total emissions, traditional point-source LDAR programmes, while necessary, risk overlooking high-impact leaks. In response, voluntary industry initiatives such as the Oil and Gas Methane Partnership 2.0

(OGMP 2.0) and the MiQ certification scheme are providing standardised frameworks for measurement-based methane reporting and independent performance certification, driving demand for more rigorous and comprehensive monitoring approaches [20,21]. Attention has therefore shifted toward detection technologies with broader spatial and temporal coverage: remote sensing platforms, continuous monitoring systems, and mobile sensing units.

Previous reviews have examined methane emissions from the oil and gas sector and assessed detection technologies across multiple scales, including remote sensing and satellite methods [22–25]. Building on this literature, the present review focuses on the applicability of these technologies to LNG operations, where facility configurations, process characteristics, and operational constraints influence monitoring requirements. It draws on a technical assessment of fugitive emissions management in the Australian LNG industry prepared by the authors for the Future Energy Exports CRC [26]. The contribution of this review lies in its LNG-specific synthesis of technical capabilities, measurement methodologies, and deployment limitations, together with consideration of how complementary technologies across monitoring scales can support measurement-informed inventories under frameworks such as OGMP 2.0.

2. Review Methodology

This article presents a narrative review of methane detection and quantification technologies relevant to LNG facilities. The main literature searches were conducted between April and August 2023, with selected additional publications incorporated during manuscript preparation and revision. No publication-year restriction was imposed on the initial searches. Scientific literature was identified through Web of Science accessed via EndNote and through OnePetro. Google searches were used to identify industry reports, supplier webpages, product catalogues, and additional technical information. Searches for component-scale sensors included terms such as “fugitive emission”, “technology readiness”, and the names of individual sensing technologies.

Literature selection involved screening titles and abstracts, reading relevant publications in full, and following their references to identify further sources. Supplier webpages and catalogues were consulted for information on sensing mechanisms, instrument specifications, commercial availability, and indicative equipment prices. Sources were selected according to their relevance to methane detection and quantification and their contribution to the discussion of monitoring technologies at component, facility, mobile, aerial, and satellite scales.

Studies conducted at LNG facilities were considered alongside evidence from other oil and gas settings because LNG-specific field measurements remain limited. When discussing findings from non-LNG settings, the review distinguishes generally applicable sensing principles and monitoring approaches from performance results that depend on facility layout, operating conditions, source characteristics, and measurement conditions.

The search and selection process was iterative and did not follow a formal systematic-review protocol. A complete numerical record of retrieved and excluded sources was not maintained. The review therefore provides a selected synthesis of relevant scientific and technical evidence rather than an exhaustive inventory of all available publications. Figure 1 summarises the search and selection process.

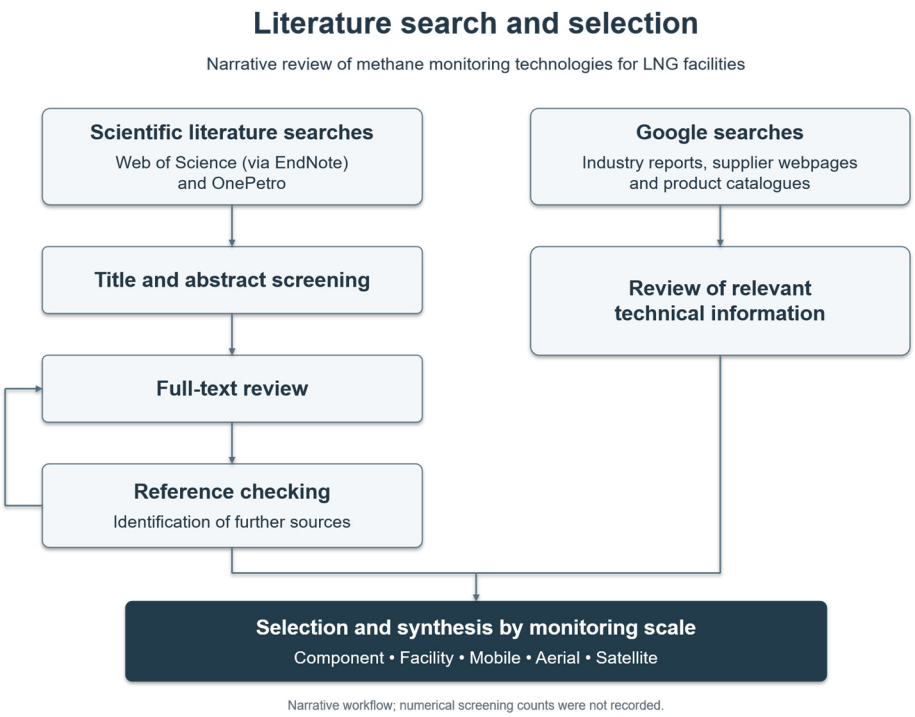


Figure 1. Literature search and selection process used in this narrative review. The diagram summarises the workflow; numerical screening counts were not recorded.

3. Component-Scale Detection Technologies

Methane emissions from individual components such as valves, flanges, compressors, and seals are a primary source of fugitive emissions in LNG facilities. Component-scale detection underpins Leak Detection and Repair (LDAR) programmes, originally developed to limit worker exposure to hazardous gases and reduce volatile organic compound emissions; methane quantification became a central objective only later. Handheld, portable, or fixed instruments measure methane concentrations and can image plumes to locate leaks. This section groups them by detection method and use case.

3.1. Proximity-Based Detection: Sniffers and Portable Sensors

Proximity-based methods use handheld instruments or fixed sensors placed near potential leak points. These tools form the backbone of many regulatory Leak Detection and Repair programmes, including the widely adopted EPA Method 21 [11], which designates a component as a "leaker" if measured concentrations exceed a specified threshold—typically 10,000 ppm. Rather than measuring leak rates directly, this approach relies on empirical correlation factors to estimate emissions based on the detected concentration. Simple and cost-effective, these methods nonetheless vary with sensor performance, environmental conditions, and operator technique. Electrochemical, metal-oxide, catalytic, and ionisation-based detectors have been developed to improve sensitivity, selectivity, and usability:

Electrochemical sensors generate an electrical signal proportional to methane concentration via a redox reaction between methane and a metal or metal-oxide electrode [27]. They are inexpensive, compact, and fast (typically <10 s), suiting them to portable or wearable multi-gas detectors. However, accuracy is limited by cross-sensitivity to gases such as CO_2 or H_2 and by dependence on temperature and humidity, and their narrow dynamic range (100 ppm to 5%) restricts use at low methane levels or in ambient air.

Metal-Oxide Semiconductor (MOS) sensors use a thin film of metal oxide that changes its electrical resistance in the presence of methane [28], proportionally to

concentration. They are inexpensive, mobile, robust, and poisoning-resistant [24] and they are commonly used in portable or indoor gas detectors. However, poor selectivity and strong temperature and humidity dependence cause drift and false readings, while long recovery times and hysteresis after high-concentration exposure hinder repeated field measurements. Their effective range (10 ppm to 1%) restricts precision or high-dilution monitoring.

Catalytic bead sensors (CBS) are widely used industrially. Two platinum-wire beads are coated with a catalyst that oxidises methane on contact [29]; the resulting heat changes the beads' electrical resistance in proportion to methane concentration. CBS are inexpensive, widely available, and fast (typically <10 s) [30]. They require oxygen and so are unsuitable for oxygen-depleted environments, and are prone to poisoning by sulphur-containing gases, silicone, and lead, and to oversaturation, which can degrade performance temporarily or permanently [31]. Their relatively high lower detection limit (~300 ppm) and limited selectivity further restrict use in ambient air monitoring or trace-level detection.

Flame Ionisation Detectors (FIDs) and Ion Mobility Spectrometry (IMS) are highly sensitive and specific. FIDs combust methane in a hydrogen flame and measure the resulting ionisation current, which is proportional to concentration [32]. With detection limits below 1 ppm, they suit trace-level measurement, but a pressurised hydrogen supply and regular calibration add to field-deployment requirements. IMS measures the mobility of ions generated when methane interacts with a gas mixture in an electric field, offering ppb-level sensitivity, faster response, and greater portability than FIDs. However, IMS can suffer from gas-phase interference [33] and may require sample pre-conditioning to maintain reliability under varying field conditions. Both are analytically robust but expensive and complex, limiting their scalability in routine LDAR programmes.

3.2. Optical Imaging and Infrared Absorption Sensors

Infrared-based sensing technologies detect or 'image' methane by measuring the radiation absorbed or emitted by the gas. Figure 2 shows the infrared spectrum of methane gas with two main peaks corresponding to the H-CH_3 stretching mode, at a wavelength of approximately 3.4 μm, and the H-CH_3 deformation modes in the 6.8–7.5 μm range. At atmospheric pressure, these lines are pressure-broadened into unresolved bands. Water vapour is a particular challenge: its absorption overlaps key methane bands near 1.7 μm and 3.4 μm, risking interference in the humid marine environments typical of coastal LNG terminals. These approaches allow non-contact, line-of-sight plume detection, making them effective for screening inaccessible equipment, large areas, or hazardous environments. The two main variants are optical gas imaging (OGI) and infrared absorption sensors.

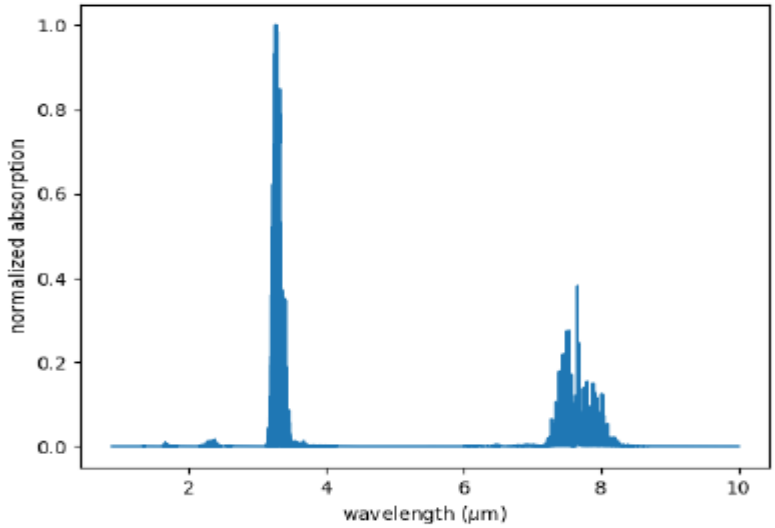


Figure 2. Infrared absorption spectrum of methane gas at 296 K and 1 atm [34,35].

Optical gas imaging (OGI) cameras detect, image, and quantify gas leaks in real time. They are passive devices that image the differential absorption of background infrared radiation by the plume, producing a visual image of leak location and size [36]. They detect leaks at distances of up to several hundred metres, which is valuable in LNG facilities and at elevated or hazardous locations where manual inspection is difficult.

As passive devices, OGIs depend on sufficient background infrared radiation and adequate plume-to-background temperature contrast (ΔT), which varies with season and site, limiting effectiveness in low light, fog, rain, or at night. For example, detection thresholds can range from as low as 43 ppm (ΔT = −30 °C, 0.3 m plume) to as high as 31,496 ppm (ΔT = 2 °C, 0.025 m plume) [37]. Quantification of leak rates using OGI involves estimating the path-integrated concentration (ppm-m) (note on the ppm-m unit: a 5 ppm-m concentration over a one-metre column indicates a 5 ppm concentration anywhere in the 1 metre layer, while 5 ppm-m over a 5-metre column indicates 1 ppm inside the 5-metre layer) and dividing by plume length, which adds uncertainty, requires assumptions about plume geometry, and is not standardised. OGI systems are also expensive and require skilled operators [38,39]. These factors limit standalone use for continuous monitoring or quantitative inventories.

Infrared absorption sensors use the absorption of infrared radiation by methane to detect its presence [40]. An infrared source and detector are separated by a gas sample cell; as shown in Figure 2, methane absorbs specific wavelengths [41], which reduces the amount of radiation that reaches the detector. High-resolution techniques such as tunable diode laser absorption spectroscopy (TDLAS) operate at reduced pressure to resolve individual lines, enabling species-specific, interference-free detection. Some hyperspectral sensors also use the short-wave infrared (SWIR) peaks centred at 1.7 μm and 2.3 μm to achieve higher spectral resolution. Deployed in fixed or portable form, they are valued for fast response (typically <10 s) and low cost, suiting general multi-gas detection [42].

The detection range of infrared absorption sensors is broad (10 to 1,000,000 ppm), and a 10 ppm lower limit is adequate for low-level detection, but sensitivity to temperature and humidity and cross-sensitivity to ethane, propane, carbon dioxide, and water vapour reduce accuracy under ambient conditions, making them best suited to controlled or semi-enclosed settings. In long-term deployments, fouling and degradation of optical windows by dust, condensation, and chemical contamination progressively attenuate the signal, requiring regular cleaning and recalibration.

3.3. Laser and Photoacoustic Spectroscopy

Laser-based and photoacoustic techniques provide high-resolution, highly selective measurements of methane. They are increasingly used in research, emissions validation, and advanced LDAR campaigns, quantifying methane at trace levels with minimal cross-sensitivity.

Tunable diode laser absorption spectroscopy (TDLAS) leverages the selective absorption of laser light by methane molecules to generate a measurable signal. Unlike broadband infrared sensors, which measure total attenuation across multiple bands, TDLAS scans a narrow tuneable laser across a single methane absorption line and operates at low pressure to avoid pressure broadening, giving highly accurate, specific quantification [43,44]. This selectivity reduces cross-sensitivity to interfering gases such as CO_2 and ethane compared to broadband IR sensors; however, water vapour remains a source of interference, particularly at high humidity (RH > 70%), where overlapping absorption features near methane lines can affect measurement accuracy. TDLAS gives real-time data with sub-second response and is less susceptible to temperature and humidity than broadband sensors. It can, however, be cost-prohibitive, and optical alignment is critical on mobile or UAV platforms where vibration and exposure affect performance. Its range (typically 1 ppm to 5%) suits leak detection but not extremely dilute or concentrated plumes.

Photoacoustic spectroscopy (PAS) detects methane by measuring acoustic waves generated when methane molecules absorb modulated laser light. The pressure changes are picked up by sensitive microphones or cantilevers, allowing ultra-low detection limits—as low as 0.1 ppb—with excellent specificity [45]. PAS accuracy is sensitive to humidity, temperature, and gas composition, which perturb the non-radiative relaxation process, so field calibration or algorithmic correction is required—a drawback for long-term unattended deployment. PAS systems are also more expensive and bulkier, need precise optical and mechanical alignment, and respond slowly (typically several seconds), limiting use on rapidly fluctuating plumes or mobile surveys. Their range (1 ppb to ~100 ppm) suits background monitoring or tracer studies rather than high-concentration leak quantification.

Across the detection techniques reviewed, sensitivity to ambient temperature and humidity is a recurring challenge. Among these, TDLAS offers relatively greater robustness through its narrow-line selectivity and analytical correction capabilities, while closed sampling systems are inherently less exposed to environmental variability than open-path techniques. In practice, no single technique is fully immune, and cross-technology validation and careful site characterisation remain important when deploying sensors outdoors.

3.4. Acoustic Detection Methods

Acoustic detection identifies gas leaks by capturing the ultrasonic “hissing” sound produced when pressurised gas escapes through fittings, valves, or pipelines. Microphone arrays record these high-frequency signals and, combined with an optical camera, generate a visual overlay of the approximate leak location, allowing operators to navigate complex facilities and localise suspect components quickly. A representative commercial implementation is the Distran Ultrasonic Camera, which has been applied in oil, gas, and LNG facilities.

The technique offers several operational advantages. Acoustic cameras are portable, non-intrusive, and quick to deploy, suiting them to screening many components in congested environments where a line-of-sight to a plume is unavailable. Unlike optical gas imaging, they can reveal leaks partially obscured by equipment, helping prioritise maintenance and directing operators to locations warranting closer inspection.

However, the method has significant limitations. Acoustic detection is not methane-specific, as it responds to any pressurised gas release such as air, CO_2, or steam. It is also vulnerable to false positives generated by reflective surfaces, ambient noise from background machinery, or adverse weather conditions. Acoustic leak-rate quantification is also new, with limited independent verification—a likely barrier to regulatory adoption. Effective use therefore requires trained operators and follow-up verification with methane-specific methods such as OGI or spectroscopy.

Advanced ultrasonic imaging systems cost tens of thousands of USD per unit, generally more than basic sniffers but less than cooled OGI cameras or high-end spectroscopic systems. Cheaper handheld detectors are also available. Acoustic detection therefore adds rapid leak localisation to LDAR workflows but, given its quantification limits, remains a complementary method within an integrated framework.

3.5. Comparative Discussion

These component-scale methods represent the fundamental building blocks of all larger-scale methane detection approaches. Facility-wide sensor networks, aerial surveys, and even satellite-based instruments ultimately rely on the same core measurement principles—most notably infrared absorption spectroscopy and imaging—but are deployed on different platforms and across broader spatial scales. Recognizing this continuity is important, as the strengths and limitations observed at the component level propagate through to larger-scale applications.

The component-scale methane detection technologies discussed in Sections 3.1–3.4 vary widely in terms of sensitivity, selectivity, response time, cost, and deployment feasibility. Selecting the most appropriate technology for Leak Detection and Repair (LDAR) programmes in LNG facilities requires balancing these factors based on operational context, regulatory requirements, and the nature of the emissions being targeted.

Proximity-based sensors, such as electrochemical, metal-oxide, catalytic bead, and ionisation-based detectors, remain foundational in regulatory frameworks such as EPA Method 21 [11] due to their portability, cost-effectiveness, and ease of use. However, they rely on empirical correlations rather than direct quantification and are hindered by cross-sensitivity, limited dynamic range, and environmental variability, suiting them to routine screening of accessible components rather than reliable detection of low-level or intermittent leaks.

Infrared technologies offer non-contact detection and visual confirmation of plumes for rapid facility-scale assessment. OGI suits inaccessible or hazardous areas but depends heavily on thermal contrast, requires skilled interpretation, is expensive, and is not standardised for precise quantification. Infrared absorption sensors are cheaper and faster to deploy but are prone to cross-sensitivity (ethane, propane, CO_2, water vapour) and environmental interference in open-air settings.

Laser-based and photoacoustic methods offer the highest sensitivity and specificity among the technologies reviewed. TDLAS gives real-time measurement and is robust in variable conditions, suiting mobile or drone deployment; PAS reaches sub-ppb detection limits, but its higher cost, larger size and weight, and slower response suit stationary or research-grade deployment. Both require careful alignment and specialised training.

Acoustic detection occupies a distinct position. While some sensors purport to quantify leak rates, the method is not methane-specific, responding instead to any pressurised gas release. Its portability, rapid deployment, and ability to localise leaks in congested environments nonetheless make it a valuable first-pass screening tool, with confirmation and quantification left to spectroscopic sensors.

A comparative summary of these technologies—including their detection performance, commercial maturity, limitations, and cost—is provided in Table 1. Note that Technology Readiness Level (TRL) values follow the NASA/ESA definition (TRL 1–9) and reflect the general commercialisation stage, not readiness for LNG deployment.

Table 1. Summary of methane-sensing technologies used in component-level detection. Technologies are compared based on detection range, detection limit, Technology Readiness Level (TRL), limitations, and approximate unit cost (USD) (prices are indicative and reflect the cited sources at their recorded access dates, where applicable). TRL values reflect overall commercial maturity of the technology. Acoustic detection methods are discussed separately in Section 3.4 as complementary tools but are not included here, since they cannot provide quantitative emission rates.

Technology	Detection Range	Detection Limit	TRL	Limitations	Cost ($/Unit)
Optical gas imaging cameras	N/A	Min leak rate: 0.4 g/hr	8–9	Interpretation may require specialized training; high uncertainty in measurements	30,000–100,000 [46–48]
Ionization methods (FIDs and IMS)	0.1 ppm to 10%	100 ppb	6–9	May require careful calibration; FIDs may not be as useful for screening large areas as some of the other technologies on this list	30,000–100,000 [49,50]
Tunable diode laser absorption spectroscopy (TDLAS)	1 ppm to 5%	1 ppm	7–9	May be relatively expensive and require specialized training to operate effectively	5000–30,000 [51,52]
Photoacoustic spectroscopy	1 ppb to 100 ppm	1 ppb	5–7	Ideal for detecting low levels of methane emissions, but may be more expensive and require further development for large-scale facilities	5000–30,000 [53,54]
Infrared absorption sensors	10 ppm to 100%	5 ppm to 10 ppm	8–9	Requires careful calibration	300–2000 [55,56]
Electrochemical sensors	100 ppm to 5%	100 ppm to 1000 ppm	6–9	Limited accuracy at low concentrations; requires careful calibration; may be affected by other gases and environmental factors	500–2000 [57]
Metal oxide semiconductor	10 ppm to 1%	10 ppm to 100 ppm	7–9	Can be prone to false alarms	50–500 [58,59]
Catalytic bead sensors	300 ppm to 5%	300 ppm to 400 ppm	7–9	Requires careful calibration	~1000 [60]

The complementary roles of these technologies are illustrated by a field study at Romanian oil and gas production facilities, where FIDs, OGI, and quantitative optical gas imaging (QOGI) were combined within an LDAR programme aligned with OGMP 2.0 [61]. Screening of 3787 components identified 41 leaks above the reporting threshold, with block valves and connectors accounting for most estimated fugitive emissions. This study provides a practical example of combining component screening and quantification to inform maintenance priorities and measurement-based reporting. For LNG facilities, this approach can inform LDAR programme design, although the reported leak prevalence and source contributions require validation under LNG-specific operating conditions.

In summary, no single sensor type offers a universal solution for fugitive methane detection at the component level. Proximity-based methods are suitable for compliance and frequent inspections; infrared systems enable rapid, broad-scale leak localisation; and laser-based techniques support high-precision quantification. The most effective LDAR strategies are increasingly tiered or hybrid, combining multiple sensor modalities to cover diverse facility conditions, emission profiles, and monitoring objectives.

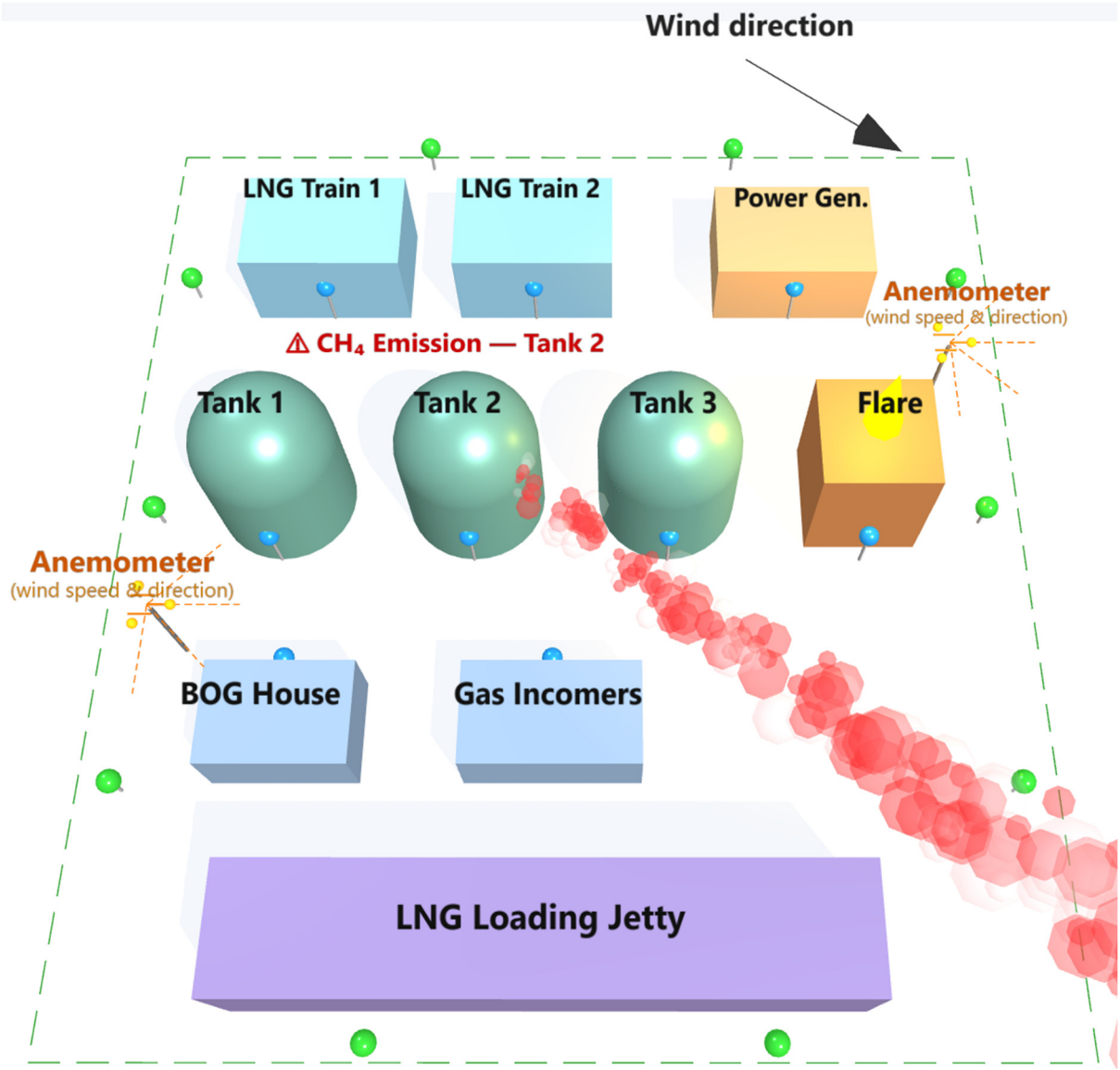
4. Facility-Scale Monitoring Systems

Leak Detection and Repair (LDAR) campaigns, run once or twice a year, are the industry standard for identifying and mitigating fugitive emissions. Being periodic, they are labour-intensive, costly, and poorly suited to intermittent or short-duration events [62]. Evidence suggests they still underestimate total emissions, particularly at LNG plants, where equipment variability, operational dynamics, and episodic leaks are common [63].

To address these limitations, continuous facility-scale monitoring systems have emerged as a promising alternative. Fixed or semi-permanent sensor arrays collect high-frequency methane and meteorological data over long periods, enabling near-real-time detection and early leak identification. They are most valuable at high-emitting facilities or those with complex leak profiles and may complement or replace conventional LDAR.

4.1. Technologies and System Capabilities

Many facility-scale monitoring concepts have been trialled, but industry-wide application remains limited; most reported examples are pilot studies or vendor demonstrations rather than established practice. Figure 3 illustrates a conceptual sensor network for an LNG liquefaction facility, showing fixed-point sensors at key functional elements and open-path sensors along the facility perimeter. The configuration is illustrative; in practice, sensor number and placement are optimised based on the distribution of potential sources and historical wind data to improve detection probability. Gas sensors and anemometers can be installed semi-permanently, recording methane concentrations alongside wind speed and direction at high frequency. Detection performance can be further improved by processing data in two stages—first filtering and averaging via edge computing using knowledge of methane dispersion, then inverting the readings using a Gaussian plume dispersion model in the cloud to identify leak existence, position, and emission rate—with results reported on a time-averaged basis, typically minutes to hours [64]. Coverage can be extended beyond the facility boundary by mounting sensors on nearby communication towers. Given that such networks are intended to operate unmanned for long periods of time under varying weather conditions, robust sensing systems are required with the capability to be automatically checked and corrected for drift via field calibration procedures [65]. Sampling methods must be optimised, with spectroscopic techniques requiring drying and/or corrections due to the presence of water vapour.



Fraction of time the source is detected depends on:

- Number of sensors deployed
- Sensor location and detection limits
- Meteorological conditions
- Duration of emission event

Legend

- Methane plume (CH_4)
- Fixed point sensor
- Fence-line sensor
- Anemometer

https://doi.org/10.3390/gases6040054

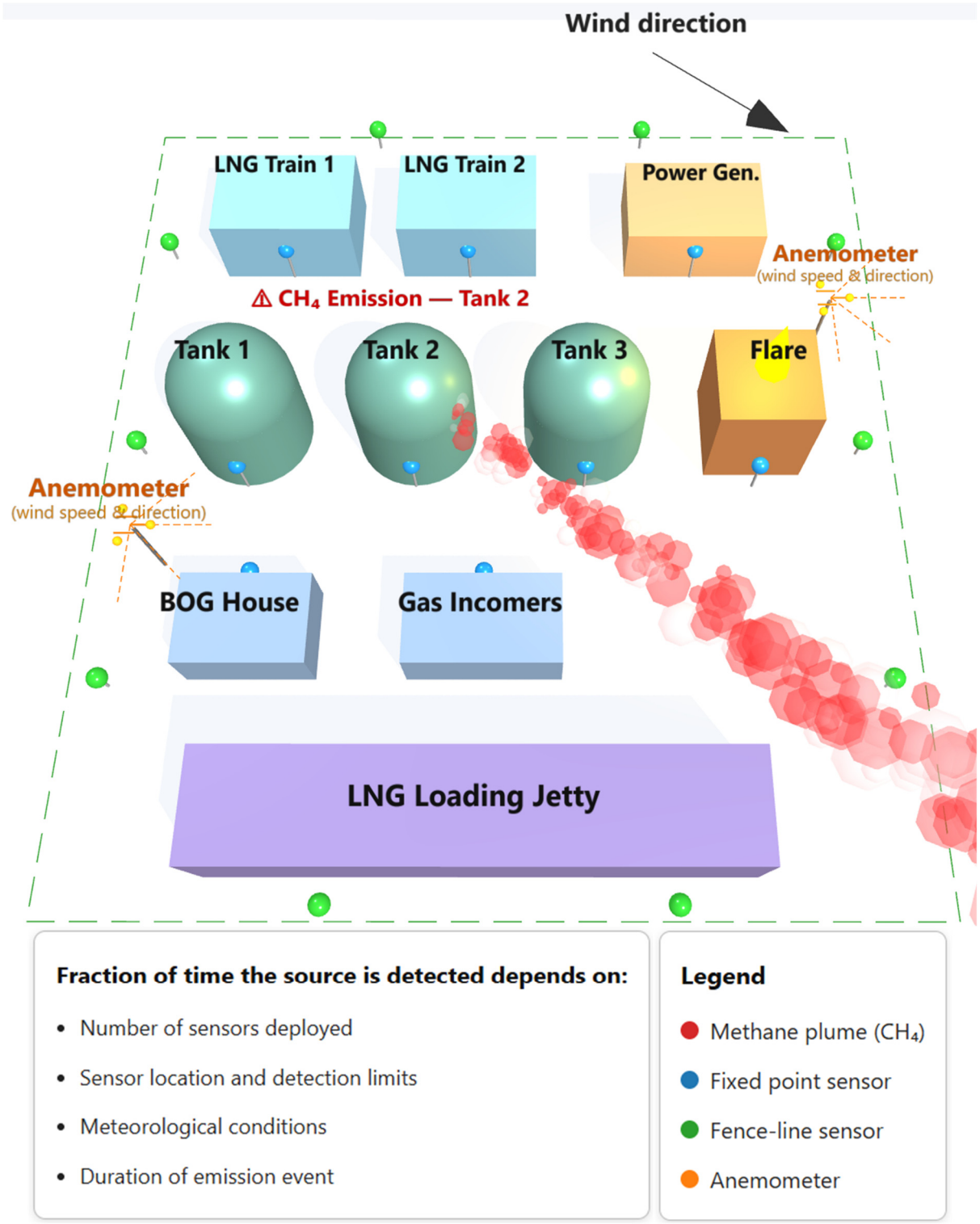


Figure 3. Conceptual schematic of a fixed methane sensor network at an LNG liquefaction facility. Fixed-point sensors (blue) and fence-line sensors (green) represent monitoring approaches discussed in Section 4.1. The facility layout, sensor locations, and methane plume near Tank 2 are illustrative and do not represent an actual industrial installation or measured emission event. Sensor number and placement require site-specific assessment of potential emission sources and meteorological conditions. Figure prepared with AI assistance.

Most commercially available continuous monitoring options use point sensors, which are inexpensive, accurate, and robust but must be distributed carefully around potential sources. OGI cameras can give direct leak rate readings, and remote sensing laser

systems provide continuous path-integrated measurements across hundreds of metres in seconds to minutes. These open-path sensors, based on Fourier Transform Infrared spectroscopy (FTIR), differential optical absorption spectroscopy (DOAS), differential absorption LIDAR (Light Detection and Ranging), or tuneable diode laser absorption spectroscopy (TDLAS), typically provide path-averaged methane concentrations (ppm—m) with uncertainties in excess of 10% [66].

A list of systems for continuous monitoring available on the market up to the year 2025 [67–69] is shown in Table 2.

Table 2. Continuous monitoring systems for methane emissions available in the market [67–69].

Brand/Model	Capabilities	Sensor	Detection Limits	Cost
Rebellion Photonics/MiniGoCGI	Multiple components only	Visible and IR spectral imaging	0.16 kg/h at 3.4 m; 0.28 kg/h at 5.9 m with 4.5 m/s winds	N/A
Sensia/Caroline SY	Multiple components only	Optical gas imaging	1.0 kg/h at 50 m; 1.8 kg/h at 100 m	€36,000
Sensia/Mileva 33F	Multiple components only	Optical gas imaging	0.35 kg/h at 100 m	€72,000
Scientific Aviation/SOOFIE	Total emissions	Metal oxide semiconductor + anemometer	1 kg/h	USD 5500 (6 sensors)
SLB/Methane Point Instrument	Total emissions	Metal oxide semiconductor + anemometer	~1 kg/h	N/A
LongPath Technologies/Emissions Sensing Network	Total emissions	Open-path frequency comb laser (TDLAS)	0.02–0.06 kg/h	N/A
Qube Technologies/Qube Emissions Monitoring System	Total emissions	Metal oxide semiconductor + anemometer	0.1–1.38 kg/h	N/A
ChampionX/SOOFIE	Total emissions	Metal oxide semiconductor + anemometer	1 kg/h	N/A
Sensirion/Nubo Sphere	Multiple components only	Photoacoustic laser spectroscopy (mid-IR)	0.8 kg/h (DL90)	N/A
Kuva Systems/Kuva (now Sensirion)	Multiple components only	SWIR camera	15 kg/h at 100 m	N/A

While systems for continuous monitoring are beginning to become available and could be effective for the quantification of long-term emissions at the facility scale, practical experience remains limited, and methods and guidelines for the correct deployment of the technology are under development.

4.2. Pilot Projects and Field Trials

A multi-institutional controlled-release experiment at the Ginninderra controlled-release facility near Canberra, Australia, from April to June 2015 provided one of the first systematic blind comparisons of methane quantification techniques under field conditions [70]. Eight quantification techniques were simultaneously assessed against a simulated methane point source release of 5.8 g/min, with participants unaware of the actual release rate. These included three tracer ratio methods, Lagrangian stochastic and footprint modelling, and atmospheric tomography with point and integrated line sensors. The majority of blind estimates were within 20% of the actual methane release rate, with the tracer ratio technique providing the closest estimates. Once the true release rate was disclosed, revised estimates improved to within 10% for most methods. An ensemble approach combining simultaneous methods reduced overall uncertainty, with the

ensemble median within 16% during the blind phase. Sensor detection limits and sampling rates emerged as the main constraints, while a hyperspectral imager successfully imaged the release from 100 m. Ginninderra remains a key reference point for the relative accuracy of atmospheric quantification methods.

The importance of continuous monitoring was also demonstrated in a U.S. pilot project tracking atmospheric trace emissions from an underground natural gas storage facility [71]. In this study, a dual-frequency comb spectrometer (DCS) was deployed on the ground with a set of 10 retroreflective mirrors, enabling 10 open paths between the laser head and each reflector. The DCS acquires high-resolution absorption spectra using an eye-safe laser, achieving 5–30 ppb accuracy; paths were measured in sequence and averaged over two to three minutes, with wind data from an anemometer 10 m away. Emissions varied by a factor of 12 to 17 daily and monthly, peaking during injection and withdrawal—evidence that continuous monitoring is needed to quantify emissions and characterise their distribution in time.

Controlled-release tests and a field pilot were conducted in Alberta (Canada) using 52 sensors installed at 16 facilities located in an area with a high density of unconventional oil and gas wells [72]. Fifteen sensors placed 50, 75, and 100 m downwind of a release source established an array detection limit of ~0.1 kg/h at up to 100 m. Over the one-year pilot, several events were detected, including vented gas and remediable leaks, resulting in significant emission reductions at the site.

Project Astra, led by the University of Texas with major oil and gas companies operating in the U.S., started in 2020 with the objective of deploying a solar-powered methane-sensing network in the Permian Basin [73]. The emission detection target was set at 5–10 kg/h, 50–100 m from the source. Four low-cost detectors (under US$5000 per device, sensitivity 100–1000 ppb) were tested in single-blind controlled-release challenges against a QC-TDLAS reference system costing over US$150,000. The results from this intercomparison study, available in an unpublished manuscript by Torres, et al. [74], indicated that the four technologies were able to detect emission rates of 5–10 kg/h with capture rates greater than 80% during nine months of operation. A digital twin simulating a 10 km^2 region minute by minute at 100 m resolution will inform the design of the Permian sensor network pilot.

These studies provide useful evidence for LNG monitoring, but most were conducted in other settings. They examined underground natural gas storage [71], unconventional oil and gas facilities [72], and upstream monitoring networks [73,74]. The Ginninderra experiment assessed measurement methods under controlled-release conditions rather than at an operating LNG facility [70]. The underlying methane-sensing principles also apply to LNG operations, and the continuous monitoring studies show how frequent measurements can reveal changes in emissions that periodic surveys may miss. However, the same sensor configurations cannot be assumed to achieve the reported detection limits, capture rates, or quantification uncertainties at LNG facilities.

Applying these methods to LNG facilities therefore requires further assessment of their performance under local conditions. Spectroscopic detection and mass-balance methods remain relevant, but their use must account for the locations and heights of emission sources, atmospheric transport, and whether measurements adequately sample the emitted plumes. Sensor placement and monitoring coverage must also suit the facility layout and operating conditions. Likewise, emission patterns measured at natural gas storage or upstream production sites do not establish how often emissions occur at LNG facilities, how long they last, or how much they contribute to total emissions. Although CO_2 tracer correlation has been evaluated at LNG facilities [9], its reliability depends on sufficiently well-known CO_2 emission rates and measurements that adequately represent both the CH_4 and CO_2 plumes. Studies conducted outside LNG facilities can therefore

guide technology selection and monitoring design, but further validation is needed to establish their performance under LNG-specific conditions.

4.3. Outlook and Limitations

Field trials in the U.S., Canada, and Australia show that continuous monitoring improves the temporal resolution and accuracy of emissions reporting, detecting both persistent and episodic emissions and supporting timely mitigation. Technologies tested in controlled and real-world settings have achieved detection limits as low as 0.1 kg/h at 100 m [72], and low-cost sensors have proven capable of detecting leaks in the 5–10 kg/h range with high capture rates [74]. Continuous monitoring is therefore a valuable complement to conventional LDAR, particularly at facilities with high variability or operational complexity.

Challenges remain. Accurate quantification and localisation require careful sensor placement, high-frequency wind data, and sophisticated modelling, and real-world performance is sensitive to environmental conditions; broader validation across facility types is needed. Most such technologies are also not yet accepted in regulatory frameworks, with standardised deployment protocols and equivalence assessments still under development—gaps that must close before continuous monitoring can enter routine LNG emissions reporting.

5. Mobile and Aerial Detection Platforms

Mobile detection offers a flexible, scalable alternative to fixed-point sensors at complex LNG facilities, rapidly surveying large areas, reaching difficult terrain, and capturing transient events missed by periodic or stationary monitoring. Ground vehicles, unmanned aerial vehicles (UAVs), and piloted aircraft operate at different altitudes and resolutions, using a range of sensors to detect, localise, and quantify emissions.

5.1. On-Road Surveys Using Vehicles

Vehicle-based systems consist of a sensor mounted on a vehicle equipped with a global positioning system (GPS) and an anemometer. This allows measurements close to facilities such as well sites or at a distance from a nearby road. A vehicle-mounted mast with multiple sampling inlets measures methane concentrations at different heights as the vehicle traverses the plume downwind of the source. These measurements, together with the wind component perpendicular to the sampling plane, are used to calculate the emission flow rate using Equation (1).

$$Q = \iint u_{\perp}(x) \cdot [C(x,z) - C_0]\, dxdz \quad (1)$$

where Q is the volumetric gas flow rate (m^3/s), $C(x,z)$ is the methane volume fraction at horizontal position x and height z within the vertical sampling plane, and C_0 is the background methane volume fraction. The sampling plane extends across the plume downwind of the source. The term $u_{\perp}(x)$ is the component of wind speed perpendicular to this plane at position x, measured by an anemometer. Typical vehicle speeds range from 8 to 16 km/h. This approach combines in situ methane concentration measurements with wind-speed measurements to estimate the emission rate and is referred to as a mass-balance method.

The Aerodyne Mobile Laboratory (AML) is an instrumented step (walk-in) van equipped with a Tuneable IR Laser Direct Absorption Spectroscopy (TDLAS) instrument suitable for measuring gas concentrations on mobile platforms. Yacovitch, et al. [75] used the AML to measure methane and ethane emissions in the Barnett Shale gas basin in Texas. Gas was sampled through an inlet tube extending from the front of the vehicle at ~2.7 m

above ground, with a scroll pump maintaining steady sub-ambient flow to the instrument. The AML was driven on public roads without site access, with some transects downwind of known emitters, including wellheads, storage tanks, compressor stations, processing and gathering stations, pipelines, and flares; onboard GPS and two anemometers supplied position and true wind speed. The distribution of detected methane emission sources peaked in the 0–5 kg/h range with a significant tail of larger emitters, and the ethane/methane molar enhancement ratio peaked at approximately 1.5% with a broad distribution between 4% and 17%, providing insight into source attribution across the Barnett Shale region.

Another instrument, the mobile Picarro G2301 Cavity Ring-Down Spectrometer (CRDS), mounted on a road vehicle equipped with an onboard GPS unit, was used in a methane survey around natural gas compressor stations in the U.S. [76]. It records time, location, and ambient methane concentration every 0.25–5.00 s and, in field tests, detected plumes of typically 3 to 20 ppm above a 1.8–2.0 ppm background.

An extensive measurement campaign was conducted as part of the Environmental Defense Fund (EDF) methane research series [77], which surveyed 36 compressor stations in gas transmission lines and nine in underground natural gas storage facilities in the U.S. A dual tracer flux method was used, which requires simultaneous measurements of methane and tracer gas concentrations. The measurements were gathered using the Picarro CRDS and the Aerodyne QC-TDLAS deployed on a mobile sampling laboratory. Two tracers (nitrous oxide and acetylene) were released at known rates from points up to 230 m apart orthogonal to the wind, bracketing the expected sources. Tracer, methane, and ethane concentrations were then measured 0.5–3 km downwind over an average of eight transects per site, and the facility-level emission rate was calculated from the known tracer release rate and the background-corrected methane-to-tracer ratio. Because tracer and methane are released close together and disperse identically, their downwind concentration ratio reflects their source emission ratio, removing the need for dispersion modelling. Site-level methane emissions varied from 2.3 up to 1000 kg/h. The largest leaks were at compressor stations, mostly from vents, valves, and engine exhaust. The distribution was highly skewed: the top 10% of sites contributed 50% of total emissions, and the bottom 50% less than 10%.

The DIAL (Differential Absorption LIDAR) mobile laboratory from the National Physical Laboratory (NPL) deploys a remote sensing laser-based instrument on a truck, allowing spatially resolved measurements of methane concentration at a stand-off distance between 50 m and 600 m with a sensitivity of 80 ppb [78]. The results of controlled-release tests have shown that this facility can measure methane leak rates in the range of 1.8 kg/h to 11 kg/h with an expanded uncertainty of 0.3 kg/h [79]. Table 3 summarises the vehicle-based sensing systems discussed above, together with their quantification methods and reported detection limits.

Table 3. Mobile sensing systems for vehicles.

Brand/Model	Sensor	Quantification Method	Detection Limits (kg/h)	Ref.
Aeris/Mira	Infrared Absorption Spectrometer	Mass-balance	0.10 (1)	[62]
Aerodyne	Tunable IR Laser Direct Absorption Spectroscopy	Dual tracer	2.00 (2)	[77]
Heath Consultants/Mobile Guard	Off-Axis Cavity Output spectrometer	Mass-balance	0.53 (1)	[62]
Licor/Li-7700	Open-Path Laser Absorption Spectrometer	Mass-balance	8.50 (1)	[62]
Picarro/G2301	Cavity Ring Down Spectrometer	Mass-balance Dual tracer	0.08 (1) 2.00 (2)	[77,80]

NPL-DIAL	Differential Absorption LIDAR	Mass-balance	1.8 [2]	[79]

[1] With 100% probability of detection; [2] based on minimum leak detected in field data.

5.2. Aerial Surveys Using Aircraft and Drones

Methane-sensing technologies based on the use of piloted aircraft have the potential to further expand the range of fugitive emissions detection from a facility to a basin level. In recent years, such aerial surveys have been able to identify and locate large emitters in several regions of the U.S. [81] and Australia [7,9]. Unmanned aerial vehicles, or drones, on the other hand, are gaining interest for their ability to fly at lower altitudes allowing them to get closer to potential leak sources that are located at heights and in areas that are more difficult or dangerous to access with conventional methods [82]. Air sampling systems and highly sensitive, multi-component gas-measuring instruments can be installed in fixed-wing aircraft or helicopters capable of carrying heavier loads for in situ determinations, and remote sensing systems can be deployed on such platforms as well. Drones are weight- and flight-time-constrained, requiring miniaturised in situ sensing equipment, but they are usually cheaper and easier to operate.

While vehicle-based methods can only scan cross-sections of a plume, aerial surveys can sample in three dimensions by conducting several transects across the convective boundary layer of a plume (mass-balance approach, Figure 4a) [83] or acquiring column-integrated methane concentration data (hyperspectral imaging approach, Figure 4b) [84]. In the mass-balance method, the methane emission rate Q is estimated by integrating the flux normal to the flight path, combining the measured concentration enhancement above background with the perpendicular wind component according to Equation (2).

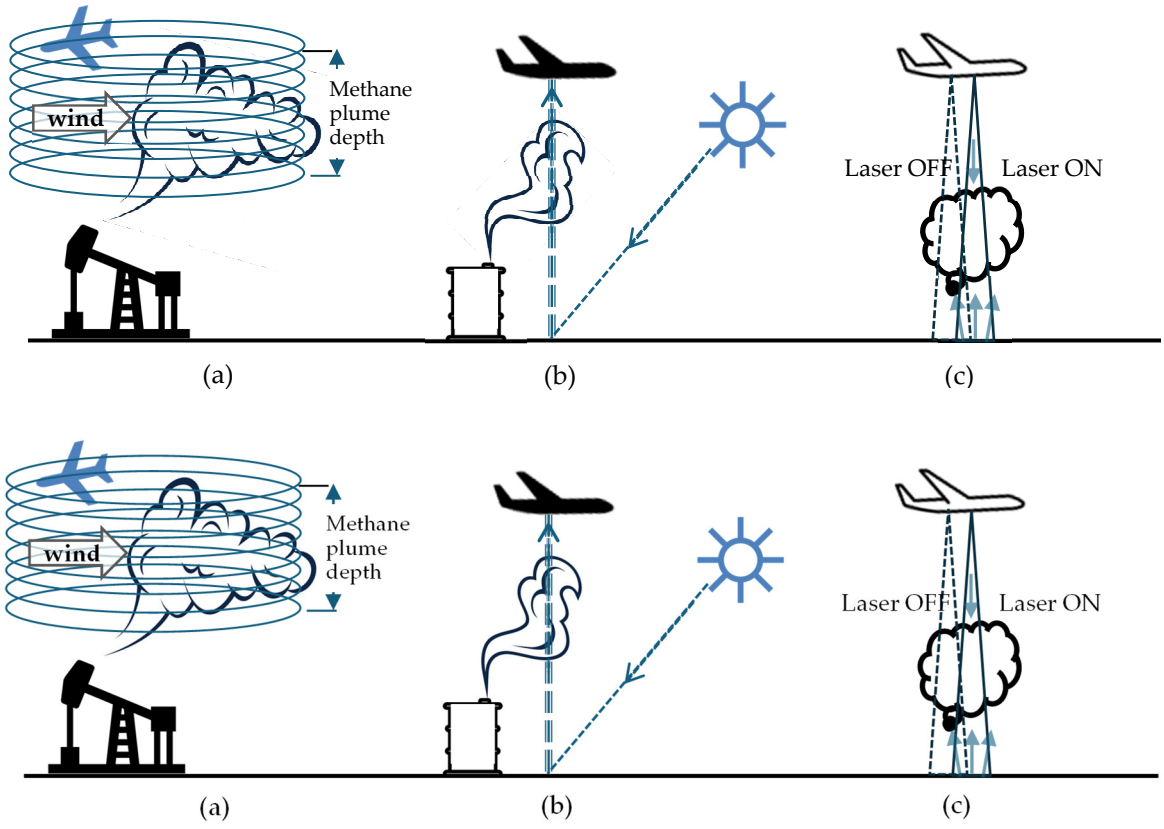


Figure 4. Illustration of airborne measurements of fugitive emission rates: (**a**) mass-balance method with in situ spectrometer [83], (**b**) hyperspectral imaging (passive remote sensing) [84], and (**c**) LiDAR scanner (active remote sensing) [85].

$$Q = \int_0^{z_{bl}} dz \oint (C - C_0)\vec{u} \cdot \hat{n}\, ds \quad (2)$$

Here, z_{bl} is the depth of the methane enhancement plume, the path integral is calculated along the plane trajectory, and the other symbols are as in Equation (1). The passive imaging method uses a spectrometer to measure methane infrared absorption in sunlight reflected from the surface. Spectrometer, optical camera, and GPS data give pixel-level estimates of excess methane column density between aircraft and the ground, which an algorithm combines with wind speed to obtain emission rates [84,86]. On UAVs rather than manned aircraft, hyperspectral imaging gains improved spatial resolution and low-altitude flexibility, though spectrally complex environments introduce band-alignment errors and geometric distortions that require correction [87]. The hyperspectral imaging method is not used over water, since water strongly absorbs infrared radiation, unless the sensor is positioned at the sun-glint angle where the water surface acts as a perfect reflector. A similar remote sensing method utilises eye-safe lasers instead of sunlight to obtain path-integrated concentration images between a back-scatterer and the aircraft (Figure 4c) as well as for range-finding (Gas-Mapping LiDAR) [85,88].

Aerial surveys for fugitive emissions are in the development phase, with some companies offering research flight services for controlled-release testing and field pilots, such as those conducted recently under the Stanford/EDF Mobile Monitoring Challenge in 2018 [62] and the Alberta Methane Field Challenge in 2019 [89]. Table 4 lists the aerial survey providers identified in this review; the following subsections describe the key drone-based and manned-aircraft systems.

Table 4. Summary of aerial fugitive emissions measurement systems.

Provider	Model	Technology/Platform	Survey Method	Detection Limit (kg/h)	Availability/Cost	Date Tested Ref.
ABB/ULC Robotics	HoverGuard	Integrated Cavity Output Spectroscopy /Drone	Raster scan	0.15 (1)	Unknown	2018, 2019 [62]
Advisian	LGR-ABB	Laser Absorption Spectroscopy/Drone	Transects with sample tube	0.06–0.10 (1)	Unknown	2019 [62]
Baker Hughes	Lumen Sky	Laser Absorption Spectroscopy/Drone	Concentric circles around equipment	0.15 (1)	Unknown/>US$5000 per measurement	2019 [62,67]
Picarro	G2210-I, G2301, G2401-m	Cavity Ring Down Spectroscopy/Drone	Upwind/downwind transects	0.15 (1)	Unknown	2017 [62]
SeekOps	SeekIR	Tunable Diode Laser Absorption Spectroscopy/UAV	Raster scan	0.02 (1)	In US/US$3000–5000 per measurement	2019 [62,67]
Ball Aerospace	N/A	Differential LiDAR/Plane	Flyover passes. Resolution: 2 m × 2 m	8.55–11.40 (1)	In US	2019 [62]
Kairos Aerospace	LeakSurveyor	Hyperspectral Imager/Plane	Pushbroom scan. Resolution 4.5 m × 4.5 m	52.00 (2)	In US/>US$15,000 per day	2017, 2019 [67,90]
Scientific Aviation	N/A	Cavity Ring Down Spectrometer/Plane	Concentric circles around facility	5.00 (1)	In US and EU/US$10,000 per day	2017, 2019 [67,90]
Bridger	Gas Mapping LiDAR (GML)	Differential LiDAR/Plane	Multiple transects Resolution: 2 m × 2 m	1–2 (1) depending on wind	In US	2021 [88,91]

Airborne Research Australia	N/A	Integrated Cavity Output Spectrometer/Plane	N/A	N/A	In Australia	2018, 2021–2023 [9,92]
Pergam	ALMA-G2 ALMA-G4	Tunable Diode Laser Absorption Spectroscopy/Helicopter-Plane	Raster scan	N/A	In Australia	2015 [93]

(1) With 100% probability of detection; (2) probability of detection unknown.

5.2.1. Drone-Based Systems

SeekOps developed the SeekIR sensor—a miniaturised, closed-cavity tunable diode laser absorption spectroscopy (TDLAS) instrument designed for mounting on drones for in situ methane concentration measurement [94]. In the Stanford/EDF Mobile Monitoring Challenge intercomparison tests [62], SeekIR achieved a 100% detection rate in all leak tests, with an estimated limit of detection of 0.019 kg/h. Quantification accuracy was more variable: only 36% of measured leak rates fell within a factor of 0.5 to 2 of the actual rate. In three selected fixed-wing tests conducted under stable atmospheric conditions, with wind speeds above 3 m/s and the preferred sampling density, absolute percentage errors ranged from 8% to 16% for release rates of 3–25 kg/h. Individual rotary-wing flux-plane tests reported absolute percentage errors ranging from approximately 1% to 88% [82].

Smith, et al. [94] describe a series of offshore measurement campaigns conducted between 2019 and 2021 at BP West of Shetland assets in the North Sea, using SeekIR sensors mounted on fixed-wing UAVs operated by FlyLogix. Data were gathered along helix trajectories of 600–800 m radius at 50–250 m altitude, giving 0.33 m spatial resolution at 30 m/s. The 2019/2020 sensor reached an in-flight detection limit of 1065 ppb, or 50 kg/h, covering only 23% of assets reporting above 1 kg/h in the 2019 EEMS dataset; actual emissions at every surveyed facility fell below this threshold. A development programme supported by the Net Zero Technology Centre (NZTC) improved the 2021 sensor to 150 ppb, or 2.5 kg/h, a twenty-fold gain covering 82% of such assets. Eighteen survey flights were flown across 11 offshore assets between 2019 and 2021.

In another field campaign in the Permian Basin over five days [83], the SeekIR drone was deployed at 33 sites with flow rates less than 10 kg/h. The drone-measured average site emission rate was 1.8 times the bottom-up estimate derived from equipment counts, a discrepancy the authors attributed to GHGRP national average emission factors that do not capture site-specific variability [83].

HoverGuard is a UAV-based technology for methane detection and quantification offered by the company ABB as part of its gas leak detection platform. It uses an Off-Axis Integrated Cavity Output Spectrometer (OA-ICOS) capable of detecting methane and ethane. The OA-ICOS sensor was developed by Los Gatos Research in California [95] and first deployed by NASA for environmental surveys in the USA and Europe on its Sensor Integrated Environmental Remote Research Aircraft (SIERRA) [96]. An off-axis beam path through a high-finesse optical cavity gives an effective path length of several kilometres, allowing sensitive spectroscopic measurements in a package light enough for UAV deployment. The technique is inherently robust and self-calibrating by rapidly switching the laser off to measure the light decay out of the cavity. Laboratory testing using calibrated methane gas standards reported methane concentration accuracy of ±1.7 ppb (1σ), while repeated measurements of a constant-composition gas sample showed precision of ±2 ppb (1σ) at a measurement rate of 1 Hz [96]. A lightweight prototype (pMGGA: prototype micro-portable Greenhouse Gas Analyzer) was drone-tested for source identification and flux quantification in two fields beside a UK gas extraction facility over five days in August and September 2018 [97]. Methane was released within

the site at two controlled rates (2.36 and 3.94 kg/h) from 0.25 m above ground, and emission rates were measured over 22 UAV surveys using a near-field Gaussian plume inversion method [97]. Across 22 UAV surveys, the known controlled-release rate fell within the derived emission-rate uncertainty interval in 19 cases. The lower and upper bounds averaged 17% and 227% of the known release rate, respectively [97]. The OA-ICOS instrument was also deployed in the Stanford/EDF Mobile Monitoring Challenge campaign by Advisian (Worley) [62,98]. It was mounted on a Vapor 55 helicopter drone (Pulse Aerospace) with a laser rangefinder and anemometer, sampling through a tube 50 feet below the aircraft. The Advisian campaign produced true-positive detections 94% of the time with an estimated detection limit of 3–5 scfh (0.057–0.095 kg/h).

In a more recent offshore deployment, two drone vendors (not disclosed by the authors) using the same TDLAS sensor technology reported site-level methane emission rates of 1 kg/h and 19 kg/h, respectively, at Woodside Energy's Shenzi platform in the Gulf of Mexico—a nineteen-fold difference attributed in part to differences in anemometer placement [99]. Protocol standardisation is therefore as critical as sensor selection, particularly offshore, where logistics limit repeat or cross-validated measurements.

5.2.2. Manned Aircraft Systems

The Airborne Laboratory for Atmospheric Research (ALAR) at Purdue University features an instrumented Beechcraft BE76 Duchess aircraft equipped with a Picarro CRDS (model G2401-m) for real-time, high-frequency measurements of CH_4, CO_2, CO, and H_2O. The ALAR was used to quantify facility emissions from natural gas-fired power plants and oil refineries [100] as well as at high-emitting point sources in a natural gas shale formation in the U.S. [101]. Flights crossed a region 1–4 km downwind of the site 8 to 14 times, each at a different altitude from near ground level to the top of the boundary layer at 50–100 m spacing, with background concentrations recorded beyond the plume edge on each transect. A mass-balance method was used to obtain the methane emission rate from the methane concentration enhancement and the wind speed data [100].

In 2017, Scientific Aviation (S.A.) deployed a Picarro CRDS on an aircraft for in situ measurements of methane over a shale gas field in the U.S. [90] to detect and quantify fugitive emissions over well pads, in a field test that also included Kairos LiDAR aerial surveys and ground measurements. From the emission-rate distribution obtained with the in situ technology by S.A. for this gas field, it was determined that, with a detection limit of 5 kg CH_4/h, the probability of detection was 100%.

The Ball Aerospace Methane Monitor uses a near-infrared absorption LiDAR system mounted on a fixed-wing aircraft for fugitive emission surveys capable of covering more than 250 km^2 in oil and gas production regions or 600 km of pipelines per day. In the Stanford/EDF Mobile Monitoring Challenge, it detected leaks above 8.55 kg/h with 100% probability, falling to 64% for smaller leaks.

Bridger Photonics offers a Gas Mapping LiDAR (GML) remote sensing system deployable by aircraft. In 2021, single-blind controlled-release tests were conducted to determine the methane detection limits of the GML technology [91]. GML detected sources ≥ 1 kg/h with ≥90% probability at 150 m above ground level (AGL), and ≥2 kg/h at 200 m AGL, under an average wind speed of 3.9 m/s; detection limits improved in low winds, likely because pooling raises the column-integrated ppm-m signal. A comprehensive measurement campaign using Bridger Photonics' GML was undertaken in 2021 to survey 508 different sites in British Columbia, including 601 active facilities and 904 active gas wells [102]. This covered 60% of active facilities and 10% of active wells in the province. Applying probability-of-detection and quantification uncertainty models, this study concluded that sources of 0.7–3.5 kg/h and 1.5–7.1 kg/h were detectable with 50% and 90% probability, respectively, depending on wind speed.

Airborne Research Australia (ARA) [103] offers research flights for airborne sensing of methane at sub-basin and facility scales using the Los Gatos Research OA-ICOS in situ sensor for CH_4 and CO_2 mounted on a motorglider. This system was deployed for the first time in Australia to quantify methane emissions in coal seam gas wells in the Surat Basin in Queensland [92,104]. Aerial LiDAR scans (Figure 4c) in the same basin were also conducted for methane remote sensing using the ALMA G2 sensor by Pergam [93] mounted on a helicopter [105].

The ARA aircraft system was subsequently deployed to evaluate airborne mass-balance and CO_2 tracer correlation methods at four Australian LNG liquefaction facilities [9]. The tracer correlation method estimates CH_4 emissions by combining measured CH_4-to-CO_2 enhancement ratios with operator estimates of CO_2 emission rates. These estimates accounted for emissions from sources including acid gas removal, power generation, LNG train fuel combustion, and flaring. Measurements collected across multiple altitudes produced CH_4 emission estimates consistent with those obtained by mass balance, with the mass-balance estimates approximately 5% higher on average. The multi-height tracer approach had lower uncertainty in this study's comparison, with a reported mean CH_4 emission uncertainty of ±30% (2σ), including uncertainty in the CO_2 emission estimates. This study therefore supports the use of CO_2 tracer correlation at LNG liquefaction facilities but also identifies important sampling requirements. CH_4-to-CO_2 ratios varied substantially with altitude, so measurements at a single height could give an unrepresentative estimate of total site emissions. Sampling across the horizontal and vertical extent of the plume helps account for differences in source location and plume dispersion. The method also depends on sufficiently accurate CO_2 emission estimates. Its potential to reduce uncertainty and simplify measurements therefore applies when these requirements are met; it should not be assumed for surveys with limited plume coverage or poorly characterised CO_2 emissions [9].

5.3. Comparative Evaluation and Practical Considerations

Ground vehicles, UAVs, and manned aircraft each occupy a distinct niche, and choosing between them trades detection sensitivity against spatial coverage, cost, and operational practicality. Vehicle-based systems offer the lowest barrier to deployment—they are mature, widely available, and capable of screening large numbers of facilities rapidly along accessible roads, with detection limits below 0.1 kg/h for the best cavity spectrometer systems. However, they are inherently constrained to road-accessible areas and cannot provide facility-wide emission totals without multiple transects and favourable wind conditions. Manned aircraft overcome the access limitation and extend coverage to basin scale, but at significantly higher cost and with detection performance that remains sensitive to flight altitude, wind speed, and data reduction methodology. UAVs sit in between—offering closer inspection and lower detection thresholds than manned aircraft and better access to elevated or restricted equipment than vehicles—but are limited by payload, endurance, and regulatory restrictions that are particularly stringent in safety-critical LNG environments.

For LNG applications specifically, no single platform currently provides a complete solution. Vehicle-based surveys are well suited to perimeter screening and road-accessible infrastructure, but cannot access offshore loading arms, elevated process equipment, or restricted zones. Manned aerial surveys can provide facility-level emission totals but lack the spatial resolution for equipment-level source attribution. UAVs offer the most promising path toward equipment-level inspection in complex LNG facilities, but regulatory approval for routine UAV operations in hazardous areas remains a significant barrier. The most effective strategies therefore combine platforms—fixed sensors for baseline monitoring, vehicles or UAVs for periodic LDAR surveys, and aerial platforms

for facility-level verification—consistent with the multi-scale framework of emerging voluntary standards such as OGMP 2.0 [21] and MiQ [20].

6. Satellite-Based Detection

Earth observation satellites, commercial and non-profit, have operated for over 50 years, and a growing number now gather atmospheric methane data used to map emissions globally. The International Energy Agency (IEA) manages the Methane Tracking Database [106], collects country-by-country estimates, and reports oil and gas emissions detected by the European Space Agency's Copernicus satellites. Among the methane remote sensing platforms, satellites offer incomparable advantages in terms of economies of scale due to their wide spatial and temporal coverage capability. Twenty years of improvement in spatial resolution and detection limits now allow satellites to image large emitters, particularly where facilities are scattered across thousands of square kilometres [107]. High detection thresholds relative to ground and low-altitude aerial methods, revisit constraints, and cloud sensitivity nevertheless prevent satellites from replacing facility-level monitoring.

6.1. Satellite Imaging and Emission Quantification Methods

Satellites use backscattered short-wave infrared (SWIR) solar radiation to obtain column-integrated methane concentrations in the atmosphere, similarly to some hyperspectral remote sensing methods applied in aerial detection [86] (Figure 4). High-resolution absorption spectroscopy and sophisticated optics give wide swaths at pixel resolutions from kilometres to tens of metres, with detection limits typically of 500–7000 kg/h aimed at identifying super-emitters. The most sensitive methane-optimised detectors, such as those in the GHGSat constellation, can reach 100 kg/h and 25 m × 25 m resolution, while WorldView-3 claims the lowest spatial resolution of 3.7 m from high-resolution SWIR measurements [108]. Most satellites are placed in a sun-synchronous, low-Earth orbit with return times on the order of one to several days, which allows them to take a series of measurements under the same observation conditions. Some agencies, such as ESA, release raw data on receipt, and processed products (level 1 radiances, level 2 methane column) are available free or by subscription through various portals [109–111] (see also [22]).

Most satellites operate their sensing systems as illustrated in Figure 5 [112]. Typically, an onboard 2D array detector collects sunlight reflected from Earth, and a high-resolution spectrometer analyses methane-induced intensity variations in the SWIR (1.65 or 2.3 μm). Some satellites operate in wide-swath mode for coverage; others use narrow-swath instruments as point source imagers. 2D plume column images are obtained at pixel sizes down to 50 m × 50 m, with each pixel within the plume mask quantified as a methane enhancement (ppb). An example of a methane plume image produced by the GHGSat constellation of satellites over an Australian mine in 2022 is shown in Figure 6.

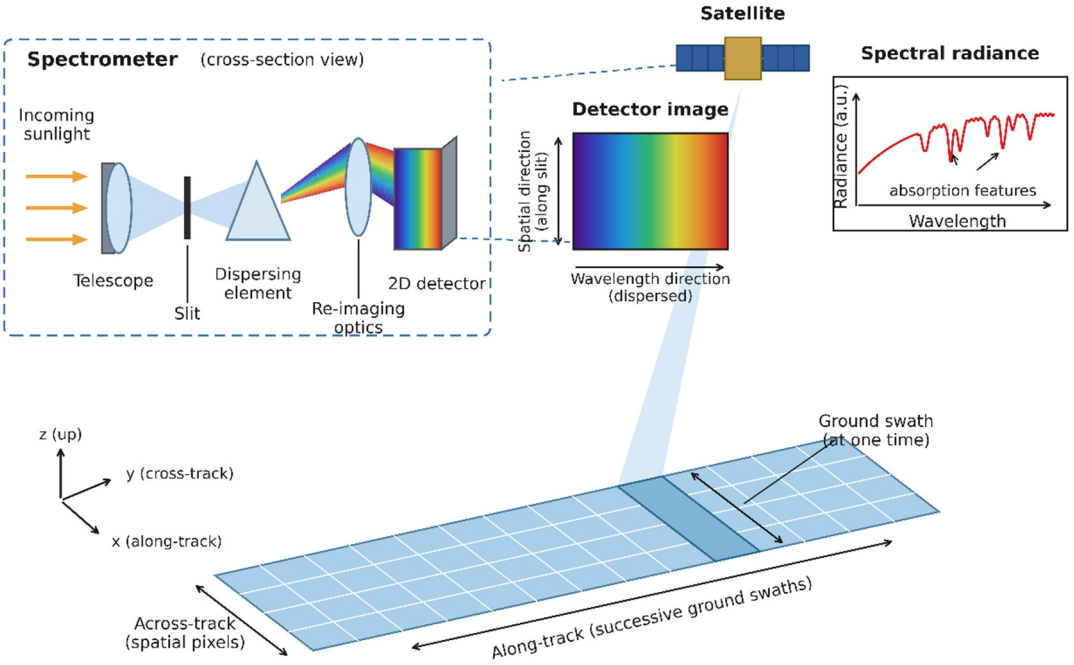


Figure 5. Illustration of a wide field of view spectrometer for GHG detection on satellites [112].

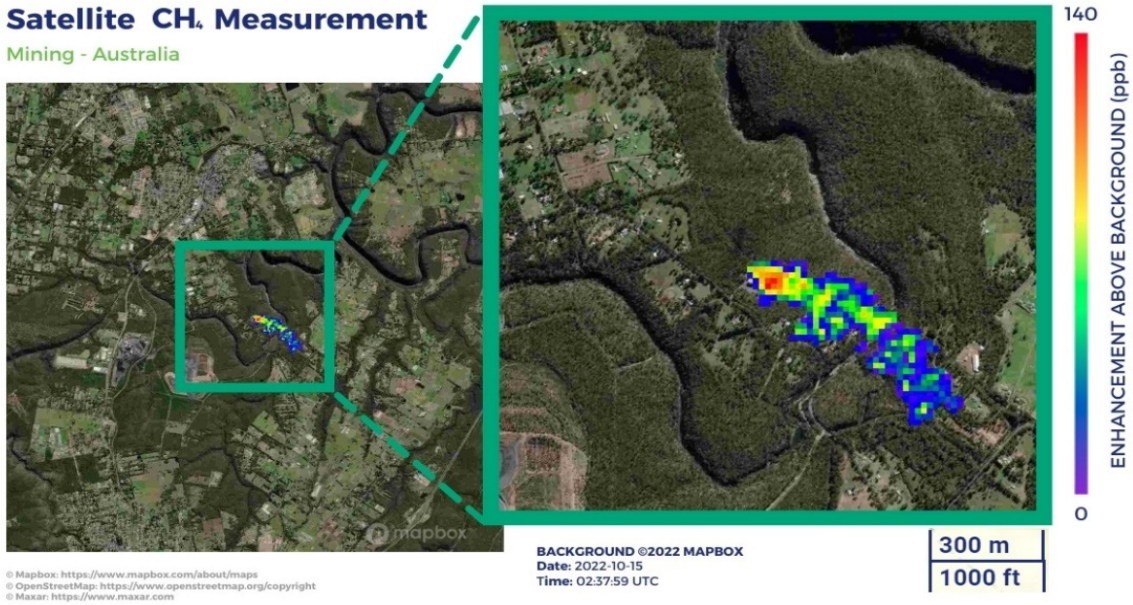


Figure 6. High-resolution image of a methane leak from a coal mine in Australia (434 kg/h) captured by GHGSat on 15/10/2022 [113]. GHGSAT Data and Products—Copyright © 2026 GHGSAT Inc. All rights reserved.

There are several different techniques to estimate the source emission rate from a quantified plume mask [22]. One of the most commonly used is the Integrated Mass Enhancement (IME) method [114], which relates the source mass flow rate Q to the total column mass enhancement in each pixel $\Delta\Omega(p)$ [kg m^{-2}] according to

$$Q = A\frac{U_{eff}}{L}\sum_{p\in M}\Delta\Omega(p) \quad (3)$$

Here, U_{eff} is the effective wind speed, L is the plume length, M is the mask of the plume, and A is the pixel area. The plume length is estimated as $L = (A \times \#M)^{0.5}$, where $\#M$

is the number of pixels within the plume mask. The effective wind speed is obtained from wind speed data measured above ground.

6.2. Satellite Instruments and Capabilities

A summary of the methane-sensing platforms deployed on satellites from 2002–25 is shown in Table 5 [22,115,116]. The first satellite capable of measuring methane, SCIAMACHY, was launched in 2002 with a near-infrared solar absorption spectrometer on board and operated until 2012, when the instrument failed. It was followed by GOSAT in 2009, which deployed a thermal and near-infrared sensor for carbon observation with higher spatial and spectral resolution (100 km^2). The TROPOspheric Monitoring Instrument (TROPOMI), launched in 2017, has a much larger spatial coverage at slightly better spatial resolution (7 km × 7 km). These first satellites, with global coverage but low spatial resolution, are classified as area flux mappers and acquire imagery continuously. On the other hand, point-source-imaging satellites such as Landsat-8, Worldview-3, Sentinel-2, and GHGSat have lower coverage but are capable of focusing on specific targets with higher resolution. GHGSat's constellation of methane-specific nano-satellites offers global coverage, imaging targets over a 12 km × 12 km field of view at 25 m × 25 m resolution, with a typical monthly revisit that can be raised to weekly or daily at additional cost. Availability nonetheless remains limited: methane-monitoring satellites average only 30–60 effective observation days per year, depending on orbit, cloud cover, and location [4]. This constraint implies that satellites alone cannot provide continuous monitoring of facilities.

Satellites provide large-scale, frequent coverage capable of locating large emitters and point sources, but measurement accuracy is uncertain: aerosols, cloud cover, terrain, and land cover around a facility all affect the result. As an example, Figure 7 presents a global methane concentration product derived from a two-week average of Sentinel-5P data, accessed through the GHGSat SPECTRA platform in August 2023. Several areas along the Pilbara coast in Western Australia, where several mega-scale LNG plants are located, display purple-red coloured pixels that nominally indicate methane concentration enhancements. Figure 7b magnifies the red square in Figure 7a: this region hosts no oil and gas facility, yet the same nominal enhancements are visible. Figure 7c shows the underlying visual layer of this region with details of the coastal and inland landscape. These apparent enhancements are a known artefact, with the intensity changes caused not by methane absorption but by water (a strong SWIR absorber) and albedo changes from sand and reef structures. As this layer is not adjusted for local context, its value lies in understanding high-level global trends rather than characterising absolute local emissions or attributing them to individual facilities, which is the role of the measurement shown in Figure 6. More generally, the same underlying satellite data may be processed according to different methodologies, so the interpretation and intercomparison of the resulting datasets, and the question of which to trust, are a wider concern for operators relying on satellite measurements. Satellite measurements are also affected by additional intrinsic limitations. Existing technologies prevent coverage of northern areas (high latitudes), mountain ranges, or ice-covered regions and offshore operations.

Table 5. Past and current methane-sensing platforms on satellites [22,115,116].

Satellite Name	Year	Spatial Resolution	Coverage	Return Time (Days)	Detection Limit (kg/h)	Ref.
SCIAMACHY	2002–2012	30 km × 60 km	Global-Area Flux Mapper	3	N/A	[117]
GOSAT	From 2009	10 km × 10 km	Global-Area Flux Mapper	3	7100	[118]

Landsat-8	From 2013	30 m × 30 m	Global-Area Flux Mapper	16	N/A	[119]
WorldView-3	From 2014	3.7 m × 3.7 m	66.5 × 112 km² targets	<1	100	[108]
Sentinel-2	2015–2017	20 m × 20 m	Global-Area Flux Mapper	2–5	1800	[120]
GHGSat-D	From 2016	50 m × 50 m	12 × 12 km² targets	1–7	1000–3000	[121]
TROPOMI	From 2017	7 km × 7 km	Global-Area Flux Mapper	1	3600–4200	[122]
GOSAT-2	From 2018	10 km × 10 km	Global-Area Flux Mapper	3	4000	[115]
PRISMA	From 2019	30 m × 30 m	30 × 30 km² targets	4	400–900	[123]
GHGSat	2021–2023	25 m × 25 m	Global 12 × 12 km² targets	1	100–200	[121]
MethaneSAT	From 2022–2025	400 m × 100 m	200 × 200 km² targets	3–4	500	[124]

Satellite data can nonetheless flag regions needing dedicated ground or airborne campaigns, complementing more accurate ground-level determinations. The first single-blind controlled methane release test campaign was conducted only recently, in 2021, with data collected from up to five point-imager satellites. Sherwin, et al. [125] reported that 71% of all emissions, ranging from 200 kg/h to 7200 kg/h, were correctly identified with a deviation of ±50% of the metered value, comparable to airplane-based remote sensing technologies. Some regions, such as Australia, are well-suited to monitoring by satellite due to their geographical position and favourable weather conditions [126]. Wang, et al. [127] demonstrated this by combining GOSAT satellite observations with ground-based atmospheric monitoring data in a high-resolution inverse modelling framework to estimate national-scale methane emissions from Australia, finding results that compare favourably with independent aircraft-based measurements. Of particular industry interest is sun-glint mode optical imaging for periodic monitoring of offshore platforms, demonstrated in preliminary Gulf of Mexico studies [128]. For LNG, high-resolution point-source imagers such as GHGSat are the most promising satellite option, their narrow-swath imagery potentially resolving facility-scale totals at large coastal terminals. Reported detection thresholds of the order of 100 kg/h, however, mean satellites remain better suited to identifying large events than to quantifying routine fugitive emissions.

The number of satellites monitoring methane has continued to grow, with several significant launches completed in 2025. GOSAT-GW, the third satellite in the JAXA GOSAT series, was successfully launched in June 2025 [129], offering improved greenhouse gas monitoring capabilities over its predecessors [130]. Sentinel-5 was launched in August 2025 [131] aboard the first MetOp Second Generation satellite, providing daily global coverage of atmospheric trace gases, including methane. GHGSat has continued to expand its commercial constellation, reaching 16 satellites by November 2025, with further launches planned through 2026 [132], aiming to provide near-daily monitoring of industrial facilities globally. These missions are expected to widen global coverage and increase the frequency of surveys targeting industrial facilities with instrumentation capable of operating with both wide and narrow swaths on demand.

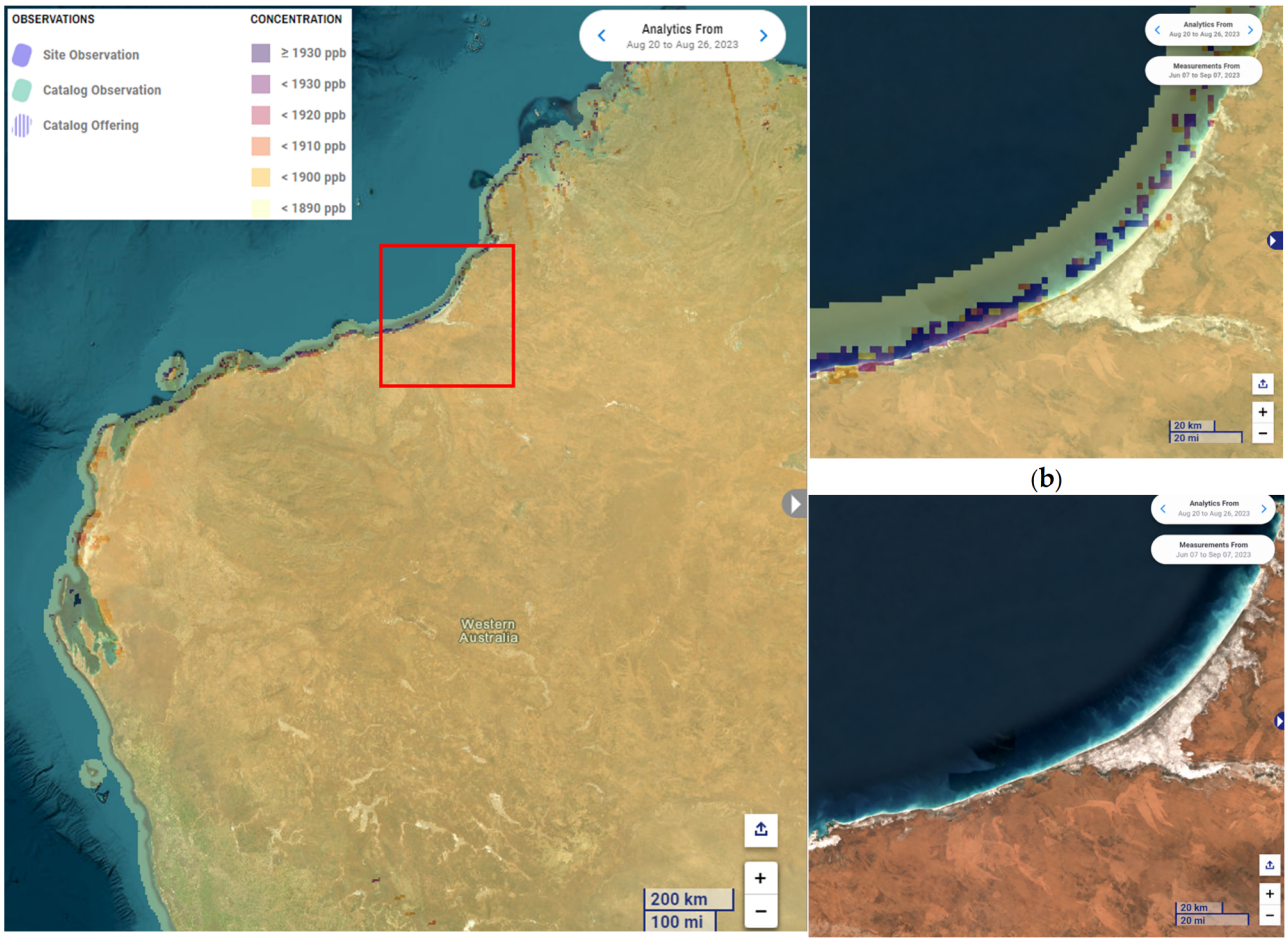


Figure 7. (**a**) Global methane concentration derived from a two-week average of Sentinel-5P data, accessed through the GHGSat SPECTRA platform, showing nominal methane concentrations along the Pilbara coast (Western Australia) on 26 August 2023. (**b**) Zoomed-in image of the area in the red square showing nominal methane enhancement pixels along the coast: this region does not contain any oil and gas facilities. (**c**) Underlying visual layer for this region showing the albedo signal from the white sand and reef structures, which, together with the presence of water, can artificially increase the apparent methane concentration measured by the satellite. GHGSAT Data and Products—Copyright © 2026 GHGSAT Inc. All rights reserved.

New developments in this area include trials with smaller, lighter satellites (one hundred kilograms in weight vs tonnes), such as the family of six Global Hyperspectral Observation Satellites (GHOSts) [133] launched in 2023. These mini satellites, developed by Orbital Sidekick Inc., are flying in a slightly lower orbit and can achieve an unprecedented spatial resolution of approximately 8 m and less than one-day revisit time.

Another important milestone in the development of satellite-based techniques is expected to be met with the launch of the Methane Remote Lidar Mission (MERLIN) [134], which will deploy active measurements of methane based on the Integrated Path Differential Absorption (IPDA) Lidar technique. IPDA uses a pulsed laser at two frequencies, one on a methane line at 1.64 μm and one at a reference wavelength with minimal absorption (analogous to Figure 4c). MERLIN, a joint French and German space mission, is expected to be launched by 2028 and, if successful, could provide global coverage during all seasons and at all times (even in total darkness) with greater accuracy and spatial resolution (≈100 m along a 50 km track) compared to passive methods.

7. Outlook and Recommendations for Fugitive Methane Detection in LNG Operations

This review has examined current and emerging technologies for detecting and quantifying fugitive methane emissions across all spatial scales relevant to LNG—from individual components and process equipment to whole facilities and basin- and global-scale satellite surveillance. As pressure grows to reduce the extent of methane emissions, which have more than 80 times the global warming potential of CO_2 over a 20-year horizon, the deployment of measurement-informed methane inventories is becoming a regulatory expectation.

Across the reviewed technologies, each detection tier offers distinct capabilities and limitations. Component-level tools such as OGI cameras, TDLAS analysers, and high-flow samplers are precise and sensitive but require manual deployment, trained operators, and site access. They suit targeted Leak Detection and Repair (LDAR) programmes but cannot cover whole sites frequently. Facility-scale fixed networks give continuous real-time data essential for identifying intermittent or operationally driven events but require careful siting, maintenance, and reliable meteorological data for accurate quantification.

Mobile and aerial platforms, including vehicle-mounted sensors, UAVs, and piloted aircraft, offer a middle ground: they can rapidly survey large areas, access difficult terrain or offshore infrastructure, and respond dynamically to suspected emission events. They are increasingly used for reconnaissance, hotspot identification, and validation, but they face flight regulations, payload constraints, environmental sensitivity, and data interpretation challenges. In the LNG context, no single platform suffices: vehicle surveys suit perimeter screening and road-accessible infrastructure but cannot access offshore loading arms, elevated process equipment, or restricted zones; manned aerial surveys give facility-level totals but lack resolution for equipment-level attribution; and UAVs, the most promising route to equipment-level inspection, await regulatory approval for routine operation in hazardous areas. At the highest scale, satellite systems offer powerful capabilities for detecting emissions over large spatial areas, identifying persistent regional sources, and tracking long-term trends. However, limitations in spatial resolution, detection sensitivity, revisit frequency, and usable observation conditions mean that satellite observations alone cannot provide the coverage required for routine reporting of methane emissions from LNG facilities. Their principal contribution is wider-area screening and the identification of large emission events, supported by complementary ground or airborne measurements for facility-level assessment.

These comparisons highlight a trade-off between broad spatial coverage and the detail needed to identify individual leaking components. They also show that high concentration sensitivity alone does not establish accurate emission-rate quantification. The appropriate combination also depends on facility configuration. At large onshore liquefaction plants, dispersed process equipment influences inspection effort and sensor-network coverage. At regasification terminals, storage, boil-off gas handling, and transfer operations require attention, including loading-arm connections that may be difficult to approach. Offshore and floating facilities impose additional constraints on access, instrument installation, and aerial deployment. These conditions should guide the selection of complementary monitoring methods.

Meeting these different monitoring needs requires complementary technologies selected for the conditions of each LNG facility. Methane management depends on integrated, multi-scale strategies combining the resolution of component tools, the continuity of fixed networks, the flexibility of mobile systems, and the reach of satellites. The most effective approaches are therefore likely to deploy continuous fixed sensors for baseline monitoring, vehicles or UAVs for periodic LDAR surveys, and aerial platforms

for facility-level verification—a multi-scale framework consistent with the measurement-based reporting standards promoted by voluntary initiatives such as OGMP 2.0 and MiQ. A recent offshore study at Woodside Energy's Shenzi platform deployed drones, aerial surveys, satellite observations, and handheld OGI simultaneously, confirming their complementarity while revealing significant inter-vendor variability in drone-based estimates [99]—underscoring that protocol standardisation is as critical as technology selection. Such hybrid systems offer a pathway toward credible, measurement-informed inventories that can augment or replace emission-factor-based estimates.

The cost-effectiveness of this multi-scale approach should be assessed for the combined monitoring programme. Each method contributes different information, so equipment prices or costs per survey alone cannot establish the most cost-effective combination. The value of adding a method depends on the monitoring gaps it addresses, the information already available, and whether it supports timely corrective action. An economic assessment would therefore require deployment and operating costs, survey frequency, detection and quantification performance, and resulting emission reductions under representative LNG conditions. The available evidence does not support a universal cost-effectiveness ranking across technologies and LNG facilities.

Beyond cost-effectiveness, the deployment of integrated monitoring programmes also depends on regulatory acceptance, access to validation infrastructure, and trained personnel. Regulatory frameworks often lag technological capability: many jurisdictions require formal protocols, equivalence testing, and field validation before recognising new methods. International initiatives such as the Oil and Gas Methane Partnership (OGMP) 2.0 and Veritas provide methodological guidance, but cross-border harmonisation and alignment with national inventory systems remain incomplete.

Many regions lack validation infrastructure—controlled-release testing grounds, calibration equipment, and independent verification laboratories—making it difficult to evaluate sensor performance under realistic conditions. Operator training is also often overlooked despite being critical to LDAR deployment and data interpretation. Mobile labs, testing consortia, and international collaboration are important steps toward closing these gaps.

The following recommendations address the limitations identified in this review, particularly the shortage of LNG-specific validation, gaps in monitoring coverage, requirements for regulatory acceptance, and difficulties in comparing and reconciling emission estimates:

1. Establish standardised field validation protocols for LNG applications. The studies discussed in Section 4.2 provide useful performance benchmarks, but most were conducted outside LNG facilities. Controlled-release tests and field comparisons under representative LNG conditions should assess detection probability, quantification uncertainty, and performance across different source locations, emission rates, and meteorological conditions.
2. Develop monitoring strategies that combine complementary technologies. The comparisons in Sections 3.5, 4.3, and 5.3 show that component surveys, fixed networks, and mobile or aerial measurements provide different levels of source identification, temporal coverage, and facility-wide quantification. Monitoring programmes should assign each technology a defined role and evaluate whether the combined measurements provide sufficient coverage for the facility. Satellite observations should be used where their detection capabilities and observation conditions are suitable, taking account of the limitations discussed in Section 6.
3. Develop clear criteria for accepting alternative monitoring methods. The regulatory discussion in the Introduction and the deployment limitations identified in Section 4.3 show the need to connect technical performance with reporting requirements.

Evaluation should consider detection probability, quantification uncertainty, survey frequency, and source coverage, rather than instrument sensitivity alone. These criteria would provide a clearer basis for assessing whether alternative methods meet the intended monitoring objective.

4. Expand access to measurement facilities that support LNG-specific validation. The limited LNG field evidence discussed in Section 4.2 highlights the need for more testing at operating facilities and under representative controlled-release conditions. Shared test facilities, mobile reference instruments, and collaborative measurement campaigns could help operators and technology developers evaluate performance across different LNG layouts and operating conditions.
5. Improve the transparency and reconciliation of emission measurements. The differences between measurement-based estimates and reported inventories discussed in the Introduction, together with the variability between monitoring approaches discussed in Sections 4 and 5, support the need for comparisons made over consistent periods and facility boundaries. Published datasets should include measurement conditions, source coverage, and uncertainty estimates so that differences between component-level and facility-level results can be investigated.
6. Evaluate monitoring coverage for intermittent and difficult-to-access fugitive emissions. The access limitations of component surveys and the temporal variability discussed in Sections 3–5 indicate that some emissions may be missed by periodic inspections. Monitoring programmes should assess how source accessibility, event duration, and survey frequency affect detection and use complementary methods where routine inspections provide insufficient coverage.

As methane emissions become increasingly important to global climate mitigation efforts, the LNG industry is uniquely positioned to lead by example in deploying credible, science-based approaches to emissions quantification. The technologies reviewed here are evolving rapidly, and many are ready for scaled deployment given enabling policy and robust validation. Measurement-informed inventories are not only a compliance tool but a pathway to public trust, operational efficiency, and demonstrated emissions-reduction leadership.

Author Contributions: Conceptualization, M.D.L., L.M., E.F.M., and M.L.J.; investigation, N.N.A.L., M.D.L., L.M., and K.J.; writing—original draft preparation, N.N.A.L., M.D.L., and L.M.; writing—review and editing, N.N.A.L., M.D.L., L.M., K.J., E.F.M., M.L.J., C.E.B., and B.W.E.N.; visualization, N.N.A.L. and M.D.L.; supervision, E.F.M., M.L.J., C.E.B., and B.W.E.N.; project administration, B.W.E.N.; funding acquisition, E.F.M., M.L.J., and C.E.B. All authors have read and agreed to the published version of the manuscript.

Funding: This research was supported by the Future Energy Exports Cooperative Research Centre (FEnEx CRC), whose activities are funded by the Australian Government's Cooperative Research Centres Program. The work forms part of Commonwealth Milestone 1.2.1 of the FEnEx CRC Commonwealth Grant Agreement. This is a FEnEx CRC Document 2026/20.RP0.001-FNX-MILE1049.

Data Availability Statement: No new data were created or analysed in this study. Data sharing is not applicable to this article.

Acknowledgments: During the preparation of this manuscript, the authors used Claude (Anthropic) to condense and improve the clarity of the written text, and to assist in preparing Figure 3 from an author-specified layout. The authors have reviewed and edited the output and take full responsibility for the content of this manuscript.

Conflicts of Interest: This research was supported by the Future Energy Exports Cooperative Research Centre (FEnEx CRC), whose participants include companies active in the LNG industry. E.F.M. is Chief Executive Officer of FEnEx CRC, M.L.J. is Research Director of FEnEx CRC, and C.E.B. is one of the programme leaders of FEnEx CRC; M.D.L., L.M., and B.W.E.N. hold FEnEx CRC Foundation Fellowships. The funders had no role in the selection of technologies reviewed, in the assessment of their performance, in the writing of the manuscript, or in the decision to publish.

References

1. Balcombe, P.; Speirs, J.F.; Brandon, N.P.; Hawkes, A.D. Methane emissions: Choosing the right climate metric and time horizon. *Environ. Sci. Processes Impacts* **2018**, *20*, 1323–1339. https://doi.org/10.1039/c8em00414e.
2. Smith, C.; Nicholls, Z.R.J.; Armour, K.; Collins, W.; Forster, P.; Meinshausen, M.; Palmer, M.D.; Watanabe, M. The Earth's Energy Budget, Climate Feedbacks, and Climate Sensitivity Supplementary Material. In *Climate Change 2021: The Physical Science Basis. Contribution of Working Group I to the Sixth Assessment Report of the Intergovernmental Panel on Climate Change*, Masson-Delmotte, V., Zhai, P., Pirani, A., Connors, S.L., Péan, C., Berger, S., Caud, N., Chen, Y., Goldfarb, L., Gomis, M.I., et al., Eds.; Cambridge University Press: Cambridge, UK, 2021; pp. 923–1054.
3. Lan, X.; Thoning, K.W.; Dlugokencky, E.J. *Trends in Globally-Averaged CH_4, N_2O, and SF_6 Determined from NOAA Global Monitoring Laboratory Measurements*, version 2026-10; Global Monitoring Laboratory: Boulder, CO, USA, 2022. https://doi.org/10.15138/P8XG-AA10.
4. International Energy Agency. *Global Methane Tracker Documentation—2025 Version*; International Energy Agency: Paris, France, 2025.
5. Nisbet, E.G.; Fisher, R.E.; Lowry, D.; France, J.L.; Allen, G.; Bakkaloglu, S.; Broderick, T.J.; Cain, M.; Coleman, M.; Fernandez, J.; et al. Methane Mitigation: Methods to Reduce Emissions, on the Path to the Paris Agreement. *Rev. Geophys.* **2020**, *58*, e2019RG000675. https://doi.org/10.1029/2019RG000675.
6. Jia, W.; Jia, P.; Gu, L.; Ren, L.; Zhang, Y.; Chen, H.; Wu, X.; Feng, W.; Cai, J. Quantification of methane emissions from typical natural gas stations using on-site measurement technology. *J. Pipeline Sci. Eng.* **2025**, *5*, 100229. https://doi.org/10.1016/j.jpse.2024.100229.
7. Innocenti, F.; Robinson, R.; Gardiner, T.; Howes, N.; Yarrow, N. Comparative Assessment of Methane Emissions from Onshore LNG Facilities Measured Using Differential Absorption Lidar. *Environ. Sci. Technol.* **2023**, *57*, 3301–3310. https://doi.org/10.1021/acs.est.2c05446.
8. Brandt, A.R.; Heath, G.A.; Cooley, D. Methane Leaks from Natural Gas Systems Follow Extreme Distributions. *Environ. Sci. Technol.* **2016**, *50*, 12512–12520. https://doi.org/10.1021/acs.est.6b04303.
9. Lunt, M.F.; Harris, S.J.; Hacker, J.; Joynes, I.; Robertson, T.; Thompson, S.; France, J.L. An evaluation of airborne mass balance and tracer correlation approaches to estimate site-level CH_4 emissions from LNG facilities using CO_2 as a tracer of opportunity. *Atmos. Meas. Tech.* **2025**, *18*, 4413–4431. https://doi.org/10.5194/amt-18-4413-2025.
10. Australian Government. *National Greenhouse and Energy Reporting (Measurement) Determination 2008*; Compilation No. 14. 2022. Australian Government: Canberra, Australia, 2022.
11. U.S. Environmental Protection Agency. *Protocol for Equipment Leak Emission Estimates*; U.S. Environmental Protection Agency: Washington, DC, USA, 1995.
12. Kangas, P.; Roberts, P.; Smithers, B.; Vaskinen, K.; Caico, C.; Tiupper, P.; Negroni, J.; Gelpi, L.; Juery, C.; Gonzalez, L.; et al. *Techniques for Detecting and Quantifying Fugitive Emissions—Results of Comparative Field Studies*; CONCAWE: Brussels, Belgium, 2015.
13. Kangas, P.; Megaritis, T. *Results of a Comparative Pilot Field Test Study of a First Generation Quantitative Optical Gas Imaging (QOGI) System*; CONCAWE: Brussels, Belgium, 2020.
14. U.S. Environmental Protection Agency. *Determination of Volatile Organic Compound and Greenhouse Gas Leaks Using Optical Gas Imaging*; U.S. Environmental Protection Agency: Washington, DC, USA, 2021**.**
15. Fox, T.A.; Ravikumar, A.P.; Hugenholtz, C.H.; Zimmerle, D.; Barchyn, T.E.; Johnson, M.R.; Lyon, D.; Taylor, T. A methane emissions reduction equivalence framework for alternative leak detection and repair programs. *Elem.-Sci. Anthr.* **2019**, *7*, 30. https://doi.org/10.1525/elementa.369.
16. Kemp, C.E.; Ravikumar, A.P. New Technologies Can Cost Effectively Reduce Oil and Gas Methane Emissions, but Policies Will Require Careful Design to Establish Mitigation Equivalence. *Environ. Sci. Technol.* **2021**, *55*, 9140–9149. https://doi.org/10.1021/acs.est.1c03071.

17. Alvarez, R.A.; Zavala-Araiza, D.; Lyon, D.R.; Allen, D.T.; Barkley, Z.R.; Brandt, A.R.; Davis, K.J.; Herndon, S.C.; Jacob, D.J.; Karion, A.; et al. Assessment of methane emissions from the U.S. oil and gas supply chain. *Science* **2018**, *361*, 186–188. https://doi.org/10.1126/science.aar7204.
18. Shen, L.; Jacob, D.J.; Gautam, R.; Omara, M.; Scarpelli, T.R.; Lorente, A.; Zavala-Araiza, D.; Lu, X.; Chen, Z.; Lin, J. National quantifications of methane emissions from fuel exploitation using high resolution inversions of satellite observations. *Nat. Commun.* **2023**, *14*, 4948. https://doi.org/10.1038/s41467-023-40671-6.
19. U.S. Department of Energy. Methane Observation Networks with Innovative Technology to Obtain Reductions. Available online: https://arpa-e.energy.gov/technologies/programs/monitor (accessed on 2 April 2023).
20. MiQ. MiQ Certification. Available online: https://miq.org/ (accessed on 14 June 2026).
21. United Nations Environment Programme. Oil and Gas Methane Partnership 2.0. Available online: https://www.ogmpartnership.org/ (accessed on 14 June 2026).
22. Jacob, D.J.; Varon, D.J.; Cusworth, D.H.; Dennison, P.E.; Frankenberg, C.; Gautam, R.; Guanter, L.; Kelley, J.; McKeever, J.; Ott, L.E.; et al. Quantifying methane emissions from the global scale down to point sources using satellite observations of atmospheric methane. *Atmos. Chem. Phys.* **2022**, *22*, 9617–9646. https://doi.org/10.5194/acp-22-9617-2022.
23. Fox, T.A.; Barchyn, T.E.; Risk, D.; Ravikumar, A.P.; Hugenholtz, C.H. A review of close-range and screening technologies for mitigating fugitive methane emissions in upstream oil and gas. *Environ. Res. Lett.* **2019**, *14*, 053002. https://doi.org/10.1088/1748-9326/ab0cc3.
24. Dey, A. Semiconductor metal oxide gas sensors: A review. *Mater. Sci. Eng. B* **2018**, *229*, 206–217. https://doi.org/10.1016/j.mseb.2017.12.036.
25. Aldhafeeri, T.; Tran, M.-K.; Vrolyk, R.; Pope, M.; Fowler, M. A Review of Methane Gas Detection Sensors: Recent Developments and Future Perspectives. *Inventions* **2020**, *5*, 28. https://doi.org/10.3390/inventions5030028.
26. Di Lorenzo, M.; McElroy, L.; Ling, N.; Jeong, K.; Johns, M.L.; May, E.F. *Improving Fugitive Emissions Management in the Australian LNG Industry*; Future Energy Exports CRC: Crawley, Australia, 2023.
27. Simões, F.R.; Xavier, M.G. Electrochemical sensors. In *Nanoscience and its Applications*; William Andrew Publishing: Norwich, NY, USA, 2017; pp. 155–178. https://doi.org/10.1016/B978-0-323-49780-0.00006-5.
28. Kanan, S.M.; El-Kadri, O.M.; Abu-Yousef, I.A.; Kanan, M.C. Semiconducting Metal Oxide Based Sensors for Selective Gas Pollutant Detection. *Sensors* **2009**, *9*, 8158–8196. https://doi.org/10.3390/s91008158.
29. Park, N.-H.; Akamatsu, T.; Itoh, T.; Izu, N.; Shin, W. Calorimetric Thermoelectric Gas Sensor for the Detection of Hydrogen, Methane and Mixed Gases. *Sensors* **2014**, *14*, 8350–8362. https://doi.org/10.3390/s140508350.
30. MSA. Catalytic Bead Sensors and Accessories Data Sheet. Available online: http://s7d9.scene7.com/is/content/minesafetyappliances/Catalytic%20Bead%20Sensors-Accessories%20Data%20Sheet (accessed on 23 March 2023).
31. Liu, X.; Cheng, S.; Liu, H.; Hu, S.; Zhang, D.; Ning, H. A Survey on Gas Sensing Technology. *Sensors* **2012**, *12*, 9635–9665. https://doi.org/10.3390/s120709635.
32. Holm, T. Aspects of the mechanism of the flame ionization detector. *J. Chromatogr. A* **1999**, *842*, 221–227. https://doi.org/10.1016/S0021-9673(98)00706-7.
33. An, S.; Joye, S.B. An improved chromatographic method to measure nitrogen, oxygen, argon and methane in gas or liquid samples. *Mar. Chem.* **1997**, *59*, 63–70. https://doi.org/10.1016/S0304-4203(97)00048-0.
34. Zimmerman, L. Comparison of Methane Plume Detection Using Shortwave and Longwave Infrared Hyperspectral Sensors Under Varying Environmental Conditions. Master's Thesis, Rochester Institute of Technology, Rochester, NY, USA, 2022.
35. Gordon, I.E.; Rothman, L.S.; Hill, C.; Kochanov, R.V.; Tan, Y.; Bernath, P.F.; Birk, M.; Boudon, V.; Campargue, A.; Chance, K.V.; et al. The HITRAN2016 molecular spectroscopic database. *J. Quant. Spectrosc. Radiat. Transf.* **2017**, *203*, 3–69. https://doi.org/10.1016/j.jqsrt.2017.06.038.
36. Singh, T.P.P. Use of Optical Gas Imaging for Visualizing Gas Leakage and other Thermal Camera Applications in Oil & Gas Sector. In Proceedings of the Abu Dhabi International Petroleum Exhibition & Conference, Abu Dhabi, United Arab Emirates, 11 November 2019; p. D011S011R002.
37. Zeng, Y.; Morris, J. Detection limits of optical gas imagers as a function of temperature differential and distance. *J. Air Waste Manag. Assoc.* **2019**, *69*, 351–361. https://doi.org/10.1080/10962247.2018.1540366.
38. Ravikumar, A.P.; Wang, J.; Brandt, A.R. Are optical gas imaging technologies effective for methane leak detection? *Environ. Sci. Technol.* **2017**, *51*, 718–724. https://doi.org/10.1021/acs.est.6b03906.

39. Fox, T.A.; Barchyn, T.; Hugenholtz, C. The winter gap effect in methane leak detection and repair with optical gas imaging cameras. In Proceedings of the AGU Fall Meeting Abstracts, New Orleans, LA, USA, 10–16 December 2017; pp. A41F–2355.
40. Triki, M.; Nguyen Ba, T.; Vicet, A. Compact sensor for methane detection in the mid infrared region based on Quartz Enhanced Photoacoustic Spectroscopy. *Infrared Phys. Technol.* **2015**, *69*, 74–80. https://doi.org/10.1016/j.infrared.2015.01.016.
41. Butt, M.A.; Degtyarev, S.A.; Khonina, S.N.; Kazanskiy, N.L. An evanescent field absorption gas sensor at mid-IR 3.39 μm wavelength. *J. Mod. Opt.* **2017**, *64*, 1892–1897. https://doi.org/10.1080/09500340.2017.1325947.
42. Gandhi, M.; Rowley, J.; Nelson, D.; Campbell, C. Gas Detection in Process Industry—The Practical Approach. In Proceedings of the Hazards, Edinburgh, UK, 13–15 May 2015.
43. Nadir, Z. A Model Based Iterative Reconstruction Approach to Tunable Diode Laser Absorption Tomography. PhD's Thesis, Purdue University, West Lafayette, IN, USA, 2018.
44. Wang, Y. Pipeline Laser Methane Detector Based on TDLAS Technology for In-situ Direct Measurement. *J. Phys. Conf. Ser.* **2022**, *2246*, 012025. https://doi.org/10.1088/1742-6596/2246/1/012025.
45. Yin, Y.; Ren, D.; Li, C.; Chen, R.; Shi, J. Cantilever-enhanced photoacoustic spectroscopy for gas sensing: A comparison of different displacement detection methods. *Photoacoustics* **2022**, *28*, 100423. https://doi.org/10.1016/j.pacs.2022.100423.
46. Global Test Supply. FLIR GF77 Uncooled Optical Gas Imaging Camera. Available online: https://www.globaltestsupply.com/online/flir-gf77-uncooled-optical-gas-imaging-camera (accessed on 26 June 2023).
47. Vision Aerial. Flir Workswell GIS-320 Optical Gas Imaging Payload. Available online: https://www.flir.com/en-au/discover/instruments/gas-detection/aerial-optical-gas-imaging-increases-inspection-efficiency-and-improves-safety/ (accessed on 26 June 2023).
48. Sensia. Mileva 33F. Available online: https://sensia-solutions.com/mileva-33f/ (accessed on 26 June 2023).
49. NEX Instrument. K9194XA | Yokogawa | Flame Ionization Detector (FID). Available online: https://www.nexinstrument.com/k9194xa (accessed on 26 June 2023).
50. Yu, J.; Hahne, R.M.A. Air Analysis. In *Encyclopedia of Analytical Science*; Elsevier: Amsterdam, The Netherlands, 2005; pp. 48–55. https://doi.org/10.1016/B0-12-369397-7/00009-1.
51. Daley Supply. Tunable Diode Laser Spectroscopy | TDLAS. Available onlinehttps://www.dronefly.com/products/airins-sniffer4d-nano-2-plus-multi-pass-tdlas-methane-unit (accessed on 26 June 2023).
52. ICI. Tunable Diode Laser Spectrometer | TDLAS. Available onlinehttps://buy.infraredcameras.com/products/ici-tdl-220-handheld-tunable-diode-laser-methane-ch4-gas-detection?srsltid=AYCX9vLJx7Gh5_3SsPcMF3ttmRT0IYkTLT3y19HwYEBJe9zbxppgRAMJ(accessed on 26 June 2023).
53. SIGAS. SIGAS SPTr-GAS®Analyzer. Available online: http://en.sigas-group.com/?products_11/52.html (accessed on 26 June 2023).
54. Xiao, H.P.; Zhao, J.B.; Sima, C.T.; Lu, P.; Long, Y.H.; Ai, Y.; Zhang, W.J.; Pan, Y.F.; Zhang, J.S.; Liu, D.M. Ultra-sensitive ppb-level methane detection based on NIR all-optical photoacoustic spectroscopy by using differential fiber-optic microphones with gold-chromium composite nanomembrane. *Photoacoustics* **2022**, *26*, 100353. https://doi.org/10.1016/j.pacs.2022.100353.
55. Euro-Gas. Infrared CH_4/Hydrocarbons GasSense NDIR Sensor. Available online: https://euro-gasman.com/product/methane-ch4-gassense-infrared-ch4-gas-sensor-with-transmitter/ (accessed on 26 June 2023).
56. CO2Meter. Cubic CU-SJH-5 Infrared Methane Gas Sensor. Available online: https://www.co2meter.com/en-au/products/infrared-methane-ch4-gas-sensor (accessed on 26 June 2023).
57. Alphasense-Ametek. Electrochemical Sensor Technology. Available online: https://www.alphasense.com/products/electrochemical/ (accessed on 26 June 2023).
58. Euro-Gas. Komyo Kitagawa SC-403 Semiconductor Gas Sensor for Methane. Available online: https://euro-gasman.com/product/methane-ch4-semiconductor-gas-sensor/ (accessed on 26 June 2023).
59. Figaro. TGS 3870-F00—For the Detection of Both Methane and Carbon Monoxide. Available online: https://www.figarosensor.com/product/docs/tgs3870-f00_product%20infomation%28fusa%29_rev03.pdf (accessed on 26 June 2023).
60. Drager. Catalytic Bead DrägerSensor. Available online: https://www.draeger.com/en_aunz/Products/Catalytic-Bead-DraegerSensors#Overview (accessed on 27 June 2023).
61. Suditu, S.; Dumitrache, L.; Branoiu, G.; Dragut, S.; Eparu, C.N.; Stan, I.G.; Prundurel, A.P. A Case Study on Advanced Detection and Management of Fugitive Methane Emissions in the Romanian Oil and Gas Sector. *Sustainability* **2025**, *17*, 11359. https://doi.org/10.3390/su172411359.

62. Ravikumar, A.P.; Sreedhara, S.; Wang, J.F.; Englander, J.; Roda-Stuart, D.; Bell, C.; Zimmerle, D.; Lyon, D.; Mogstad, I.; Ratner, B.; et al. Single-blind inter-comparison of methane detection technologies—Results from the Stanford/EDF Mobile Monitoring Challenge. *Elem.-Sci. Anthr.* **2019**, *7*, 37. https://doi.org/10.1525/elementa.373.
63. Vaughn, T.L.; Bell, C.S.; Pickering, C.K.; Schwietzke, S.; Heath, G.A.; Pétron, G.; Zimmerle, D.J.; Schnell, R.C.; Nummedal, D. Temporal variability largely explains top-down/bottom-up difference in methane emission estimates from a natural gas production region. *Proc. Natl. Acad. Sci. USA* **2018**, *115*, 11712–11717. https://doi.org/10.1073/pnas.1805687115.
64. Chakrabarti, A.; Dauphin, M.; Andrews, B.; Zielinski, L.; Rashid, K.; Yuan, J.; Speck, A. Rapid Detection of Methane Super-Emitters Through Advanced Interpretation. In Proceedings of the ADIPEC, Abu Dhabi, United Arab Emirates, 31 October–3 November 2022.
65. Richardson, S.J.; Miles, N.L.; Davis, K.J.; Lauvaux, T.; Martins, D.K.; Turnbull, J.C.; McKain, K.; Sweeney, C.; Cambaliza, M.O.L. Tower measurement network of in-situ CO2, CH4, and CO in support of the Indianapolis FLUX (INFLUX) Experiment. *Elem. Sci. Anthr.* **2017**, *5*, 59. https://doi.org/10.1525/elementa.140.
66. U.S. Environmental Protection Agency. *EPA Handbook: Optical Remote Sensing for Measurement and Monitoring of Emissions Flux*; U.S. Environmental Protection Agency: 2011.
67. Carbon Limits AS. *Overview of methane detection and measurement technologies for offshore applications*; Norwegian Oil and Gas Association: Washington, DC, USA, 2020.
68. Chen, Z.; El Abbadi, S.H.; Sherwin, E.D.; Burdeau, P.M.; Rutherford, J.S.; Chen, Y.; Zhang, Z.; Brandt, A.R. Comparing Continuous Methane Monitoring Technologies for High-Volume Emissions: A Single-Blind Controlled Release Study. *ACS ES&T Air* **2024**, *1*, 871–884. https://doi.org/10.1021/acsestair.4c00015.
69. LongPath Techonologies. LongPath Techonologies Solution. Available online: https://www.longpathtech.com/solutions (accessed on 5 July 2026).
70. Feitz, A.; Schroder, I.; Phillips, F.; Coates, T.; Negandhi, K.; Day, S.; Luhar, A.; Bhatia, S.; Edwards, G.; Hrabar, S.; et al. The Ginninderra CH_4 and CO_2 release experiment: An evaluation of gas detection and quantification techniques. *Int. J. Greenh. Gas Control* **2018**, *70*, 202–224. https://doi.org/10.1016/j.ijggc.2017.11.018.
71. Alden, C.B.; Wright, R.J.; Coburn, S.C.; Caputi, D.; Wendland, G.; Rybchuk, A.; Conley, S.; Faloona, I.; Rieker, G.B. Temporal Variability of Emissions Revealed by Continuous, Long-Term Monitoring of an Underground Natural Gas Storage Facility. *Environ. Sci. Technol.* **2020**, *54*, 14589–14597. https://doi.org/10.1021/acs.est.0c03175.
72. Benko, T.; MacGregor, A.; Wen, E.; Fox, T.; Moorhouse, B. Continuous Methane Measurement: Equivalency Evaluation of Regulator-Approved Alternative Leak Detection and Repair Program in Alberta, Canada. In Proceedings of the SPE Annual Technical Conference and Exhibition, Houston, TX, USA, 3–5 October 2022.
73. The University of Texas at Austin. Project Astra. Advancing Next Generation Methane Innovation. Available online: https://energy.utexas.edu/news/new-ut-collaboration-revolutionize-way-methane-leaks-are-found (accessed on 6 April 2023)).
74. Torres, V.M.; Sullivan, D.W.; He'Bert, E.; Spinhirne, J.; Modi, M.; Allen, D.T. Field inter-comparison of low-cost sensors for monitoring methane emissions from oil and gas production operations. *Atmos. Meas. Tech.* **2022**, *preprint*. https://doi.org/10.5194/amt-2022-24.
75. Yacovitch, T.I.; Herndon, S.C.; Pétron, G.; Kofler, J.; Lyon, D.; Zahniser, M.S.; Kolb, C.E. Mobile Laboratory Observations of Methane Emissions in the Barnett Shale Region. *Environ. Sci. Technol.* **2015**, *49*, 7889–7895. https://doi.org/10.1021/es506352j.
76. Payne, B.F.; Ackley, R.; Wicker, A.P.; Hildenbrand, Z.L.; Carlton, D.D.; Schug, K.A. Characterization of methane plumes downwind of natural gas compressor stations in Pennsylvania and New York. *Sci. Total Environ.* **2017**, *580*, 1214–1221. https://doi.org/10.1016/j.scitotenv.2016.12.082.
77. Subramanian, R.; Williams, L.L.; Vaughn, T.L.; Zimmerle, D.; Roscioli, J.R.; Herndon, S.C.; Yacovitch, T.I.; Floerchinger, C.; Tkacik, D.S.; Mitchell, A.L.; et al. Methane Emissions from Natural Gas Compressor Stations in the Transmission and Storage Sector: Measurements and Comparisons with the EPA Greenhouse Gas Reporting Program Protocol. *Environ. Sci. Technol.* **2015**, *49*, 3252–3261. https://doi.org/10.1021/es5060258.
78. UK National Physical Laboratory. *DIAL for Remote Emissions Measurement*; UK National Physical Laboratory: Teddington, UK, 2023.
79. Gardiner, T.; Helmore, J.; Innocenti, F.; Robinson, R. Field Validation of Remote Sensing Methane Emission Measurements. *Remote Sensing* **2017**, *9*, 956. https://doi.org/10.3390/rs9090956.
80. Tsai, T.R.; Du, K.; Stavropoulos, B. New system for detecting, mapping, monitoring, quantifying and reporting fugitive gas emissions. *APPEA J.* **2017**, *57*, 561–566. https://doi.org/10.1071/AJ16098.

81. Cusworth, D.H.; Duren, R.M.; Thorpe, A.K.; Olson-Duvall, W.; Heckler, J.; Chapman, J.W.; Eastwood, M.L.; Helmlinger, M.C.; Green, R.O.; Asner, G.P.; et al. Intermittency of Large Methane Emitters in the Permian Basin. *Environ. Sci. Technol. Lett.* **2021**, *8*, 567–573. https://doi.org/10.1021/acs.estlett.1c00173.
82. Corbett, A.; Smith, B. A Study of a Miniature TDLAS System Onboard Two Unmanned Aircraft to Independently Quantify Methane Emissions from Oil and Gas Production Assets and Other Industrial Emitters. *Atmosphere* **2022**, *13*, 804. https://doi.org/10.3390/atmos13050804.
83. Stokes, S.; Tullos, E.; Morris, L.; Cardoso-Saldaña, F.J.; Smith, M.; Conley, S.; Smith, B.; Allen, D.T. An aerial field trial of methane detection technologies at oil and gas production sites. *Environ. Sci. Technol.* **2022**. https://doi.org/10.26434/chemrxiv-2022-g2mjt-v2.
84. Sherwin, E.D.; Chen, Y.; Ravikumar, A.P.; Brandt, A.R. Single-blind test of airplane-based hyperspectral methane detection via controlled releases. *Elem.-Sci. Anthr.* **2021**, *9*, 00063. https://doi.org/10.1525/elementa.2021.00063.
85. Amediek, A.; Ehret, G.; Fix, A.; Wirth, M.; Büdenbender, C.; Quatrevalet, M.; Kiemle, C. Performance of Charm-F—The airborne demonstrator for Merlin. *EPJ Web Conf.* **2018**, *176*, 01002. https://doi.org/10.1051/epjconf/201817601002.
86. Thorpe, A.K.; O'Handley, C.; Emmitt, G.D.; Decola, P.L.; Hopkins, F.M.; Yadav, V.; Guha, A.; Newman, S.; Herner, J.D.; Falk, M.; et al. Improved methane emission estimates using AVIRIS-NG and an Airborne Doppler Wind Lidar. *Remote Sens. Environ.* **2021**, *266*, 112681. https://doi.org/10.1016/j.rse.2021.112681.
87. Banerjee, B.P.; Raval, S.; Cullen, P.J. UAV-hyperspectral imaging of spectrally complex environments. *Int. J. Remote Sens.* **2020**, *41*, 4136–4159. https://doi.org/10.1080/01431161.2020.1714771.
88. Johnson, M.R.; Tyner, D.R.; Szekeres, A.J. Blinded evaluation of airborne methane source detection using Bridger Photonics LiDAR. *Remote Sens. Environ.* **2021**, *259*, 112418. https://doi.org/10.1016/j.rse.2021.112418.
89. Ravikumar, A.P.; Singh, D.; Barlow, B.; Robinson, C.; Funk, W. *Alberta Methane Field Challenge*; Alberta Upstream Petroleum Research Fund: Calgary, AB, Canada, 2020.
90. Schwietzke, S.; Harrison, M.; Lauderdale, T.; Branson, K.; Conley, S.; George, F.C.; Jordan, D.; Jersey, G.R.; Zhang, C.; Mairs, H.L.; et al. Aerially guided leak detection and repair: A pilot field study for evaluating the potential of methane emission detection and cost-effectiveness. *J. Air Waste Manag. Assoc.* **2019**, *69*, 71–88. https://doi.org/10.1080/10962247.2018.1515123.
91. Bell, C.; Rutherford, J.; Brandt, A.R.; Sherwin, E.; Vaughn, T.; Zimmerle, D. Single-blind determination of methane detection limits and quantification accuracy using aircraft-based LiDAR. *Elem.-Sci. Anthr.* **2022**, *10*, 00080. https://doi.org/10.1525/elementa.2022.00080.
92. Neininger, B.G.; Kelly, B.F.J.; Hacker, J.M.; Lu, X.; Schwietzke, S. Coal seam gas industry methane emissions in the Surat Basin, Australia: Comparing airborne measurements with inventories. *Philos. Trans. R. Soc. A Math. Phys. Eng. Sci.* **2021**, *379*, 20200458. https://doi.org/10.1098/rsta.2020.0458.
93. Pergam-Suisse AG. ALMA-Aerial Laser Methane Assessment. Available online: https://pergam-suisse.ch/alma#!/tab/156887121-1 (accessed on 20 April 2023).
94. Smith, B.; Buckingham, S.; Touzel, D.; Corbett, A.; Tavner, C. Development of Methods for Top-Down Methane Emission Measurements of Oil and Gas Facilities in an Offshore Environment Using a Miniature Methane Spectrometer and Long-Endurance UAS. In Proceedings of the SPE Annual Technical Conference and Exhibition, Dubai, United Arab Emirates, 21–23 September 2021.
95. Baer, D.S.; Paul, J.B.; Gupta, M.; O'Keefe, A. Sensitive absorption measurements in the near-infrared region using off-axis integrated-cavity-output spectroscopy. *Appl. Phys. B Lasers Opt.* **2002**, *75*, 261–265. https://doi.org/10.1007/s00340-002-0971-z.
96. Berman, E.S.F.; Fladeland, M.; Liem, J.; Kolyer, R.; Gupta, M. Greenhouse gas analyzer for measurements of carbon dioxide, methane, and water vapor aboard an unmanned aerial vehicle. *Sens. Actuators B-Chem.* **2012**, *169*, 128–135. https://doi.org/10.1016/j.snb.2012.04.036.
97. Shah, A.; Pitt, J.R.; Ricketts, H.; Leen, J.B.; Williams, P.I.; Kabbabe, K.; Gallagher, M.W.; Allen, G. Testing the near-field Gaussian plume inversion flux quantification technique using unmanned aerial vehicle sampling. *Atmos. Meas. Tech.* **2020**, *13*, 1467–1484. https://doi.org/10.5194/amt-13-1467-2020.
98. Amin, L. Remote Sensing for Leak Detection and Quantification. In Proceedings of the SPE Offshore Europe Conference and Exhibition, Aberdeen, UK, 3–6 September .
99. Deshpande, S.; Collins, E.; Joynes, I.; O'Keeffe, R. Methane emissions measurement insights from an Offshore Measurement, Monitoring, Reporting and Verification study. *Aust. Energy Prod. J.* **2025**, *65*, EP24038. https://doi.org/10.1071/EP24038.

100. Lavoie, T.N.; Shepson, P.B.; Gore, C.A.; Stirm, B.H.; Kaeser, R.; Wulle, B.; Lyon, D.; Rudek, J. Assessing the Methane Emissions from Natural Gas-Fired Power Plants and Oil Refineries. *Environ. Sci. Technol.* **2017**, *51*, 3373–3381. https://doi.org/10.1021/acs.est.6b05531.
101. Lavoie, T.N.; Shepson, P.B.; Cambaliza, M.O.L.; Stirm, B.H.; Karion, A.; Sweeney, C.; Yacovitch, T.I.; Herndon, S.C.; Lan, X.; Lyon, D. Aircraft-Based Measurements of Point Source Methane Emissions in the Barnett Shale Basin. *Environ. Sci. Technol.* **2015**, *49*, 7904–7913. https://doi.org/10.1021/acs.est.5b00410.
102. Johnson, M.R.; Conrad, B.M.; Tyner, D.R. Creating measurement-based oil and gas sector methane inventories using source-resolved aerial surveys. *Commun. Earth Environ.* **2023**, *4*, 139. https://doi.org/10.1038/s43247-023-00769-7.
103. Airborne Research Australia. Available online: http://www.airborneresearch.com.au/ (accessed on 18 March 2023).
104. Kelly, B.F.J.; Lu, X.; Harris, S.J.; Neininger, B.G.; Hacker, J.M.; Schwietzke, S.; Fisher, R.E.; France, J.L.; Nisbet, E.G.; Lowry, D.; et al. Atmospheric methane isotopes identify inventory knowledge gaps in the Surat Basin, Australia, coal seam gas and agricultural regions. *Atmos. Chem. Phys.* **2022**, *22*, 15527–15558. https://doi.org/10.5194/acp-22-15527-2022.
105. Day, S.; Ong, C.; Rodger, A.; Etheridge, D.; Hibberd, M.; van Gorsel, E.; Spencer, D.; Krummel, P.; Zegelin, S.; Barrett, D.; et al. *Characterisation of Regional Fluxes of Methane in the Surat Basin, Queensland—Phase 2: A Pilot Study of Methodology to Detect and Quantify Methane Sources*; CSIRO: Canberra, Australia, 2015.
106. International Energy Agency. Methane Tracker Database 2022. Available online: https://www.iea.org/reports/global-methane-tracker-2022/overview (accessed on 27 April 2023).
107. Varon, D.J.; McKeever, J.; Jervis, D.; Maasakkers, J.D.; Pandey, S.; Houweling, S.; Aben, I.; Scarpelli, T.; Jacob, D.J. Satellite Discovery of Anomalously Large Methane Point Sources From Oil/Gas Production. *Geophys. Res. Lett.* **2019**, *46*, 13507–13516. https://doi.org/10.1029/2019gl083798.
108. Sánchez-García, E.; Gorroño, J.; Irakulis-Loitxate, I.; Varon, D.J.; Guanter, L. Mapping methane plumes at very high spatial resolution with the WorldView-3 satellite. *Atmos. Meas. Tech.* **2022**, *15*, 1657–1674. https://doi.org/10.5194/amt-15-1657-2022.
109. Copernicus Australasia Regional Data Hub. The Copernicus Australiasia Regional Hub. Available online: https://www.copernicus.gov.au/home (accessed on 18 April 2023).
110. Carbon Mapper. Carbon Mapper: Accelerating Local Action Globally. Available online: https://carbonmapper.org/ (accessed on 15 April 2023).
111. GHGsat. Spectra. Available online: https://www.ghgsat.com/en/products-services/spectra/ (accessed on 14 April 2023).
112. The European Space Agency (ESA). Copernicus: Sentinel-4. Available online: https://www.eoportal.org/satellite-missions/copernicus-sentinel-4#uvn-ultraviolet-visible-near-infrared-spectrometer (accessed on 29 March 2023).
113. GHGsat. GHGSat Technology. Available online: https://www.ghgsat.com/en/technology/ (accessed on 14 April 2023).
114. Varon, D.J.; Jacob, D.J.; McKeever, J.; Jervis, D.; Durak, B.O.A.; Xia, Y.; Huang, Y. Quantifying methane point sources from fine-scale satellite observations of atmospheric methane plumes. *Atmos. Meas. Tech.* **2018**, *11*, 5673–5686. https://doi.org/10.5194/amt-11-5673-2018.
115. Cooper, J.; Dubey, L.; Hawkes, A. Methane detection and quantification in the upstream oil and gas sector: The role of satellites in emissions detection, reconciling and reporting. *Environ. Sci. Atmos.* **2022**, *2*, 9–23. https://doi.org/10.1039/d1ea00046b.
116. Gauthier, J.-F. Strength in numbers: How the different satellite systems used to monitor methane emissions from space have different, yet complementary, capabilities to help the oil and gas industry meet its decarbonisation goals. *APPEA J.* **2022**, *62*, S112–S116. https://doi.org/10.1071/aj21080.
117. Burrows, J.P.; Holzle, E.; Goede, A.P.H.; Visser, H.; Fricke, W. Sciamachy—Scanning Imaging Absorption Spectrometer For Atmospheric Chartography. *Acta Astronaut.* **1995**, *35*, 445–451. https://doi.org/10.1016/0094-5765(94)00278-t.
118. Parker, R.J.; Webb, A.; Boesch, H.; Somkuti, P.; Barrio Guillo, R.; Di Noia, A.; Kalaitzi, N.; Anand, J.S.; Bergamaschi, P.; Chevallier, F.; et al. A decade of GOSAT Proxy satellite CH4 observations. *Earth Syst. Sci. Data* **2020**, *12*, 3383–3412. https://doi.org/10.5194/essd-12-3383-2020.
119. Ehret, T.; De Truchis, A.; Mazzolini, M.; Morel, J.-M.; D'Aspremont, A.; Lauvaux, T.; Duren, R.; Cusworth, D.; Facciolo, G. Global Tracking and Quantification of Oil and Gas Methane Emissions from Recurrent Sentinel-2 Imagery. *Environ. Sci. Technol.* **2022**, *56*, 10517–10529. https://doi.org/10.1021/acs.est.1c08575.
120. Varon, D.J.; Jervis, D.; McKeever, J.; Spence, I.; Gains, D.; Jacob, D.J. High-frequency monitoring of anomalous methane point sources with multispectral Sentinel-2 satellite observations. *Atmos. Meas. Tech.* **2021**, *14*, 2771–2785. https://doi.org/10.5194/amt-14-2771-2021.
121. Jervis, D.; McKeever, J.; Durak, B.O.A.; Sloan, J.J.; Gains, D.; Varon, D.J.; Ramier, A.; Strupler, M.; Tarrant, E. The GHGSat-D imaging spectrometer. *Atmos. Meas. Tech.* **2021**, *14*, 2127–2140. https://doi.org/10.5194/amt-14-2127-2021.

122. The European Space Agency. Copernicus Sentinel Data Products—Sentinel-5 Precursor Level 2 Methane. Available online: https://sentinels.copernicus.eu/web/sentinel/data-products/-/asset_publisher/fp37fc19FN8F/content/tropomi-level-2-methane (accessed on 20 March 2023).
123. Guanter, L.; Irakulis-Loitxate, I.; Gorrono, J.; Sanchez-Garcia, E.; Cusworth, D.H.; Varon, D.J.; Cogliati, S.; Colombo, R. Mapping methane point emissions with the PRISMA spaceborne imaging spectrometer. *Remote Sens. Environ.* **2021**, *265*. https://doi.org/10.1016/j.rse.2021.112671.
124. Rohrschneider, R.R.; Wosfy, S.; Franklint, J.E.; Benmergui, J.; Soto, J.; Davis, B.D. The MethaneSAT Mission. In Proceedings of the 35th Annual Small Satellite Conference, Austin, TX, USA, 7–12 August 2021.
125. Sherwin, E.D.; Rutherford, J.S.; Chen, Y.; Aminfard, S.; Kort, E.A.; Jackson, R.B.; Brandt, A.R. Single-blind validation of space-based point-source detection and quantification of onshore methane emissions. *Sci. Rep.* **2023**, *13*, 3836. https://doi.org/10.1038/s41598-023-30761-2.
126. International Energy Agency. *Global Methane Tracker Documentation—2023 Version*; International Energy Agency: Paris, France, 2023.
127. Wang, F.; Maksyutov, S.; Janardanan, R.; Ito, A.; Morino, I.; Yoshida, Y.; Someya, Y.; Tohjima, Y.; Kelly, B.F.J.; Kaiser, J.W.; et al. Methane emissions from Australia estimated by inverse analysis using in-situ and Satellite (GOSAT) atmospheric observations. *GISci. Remote Sens.* **2025**, *62*, 2488595. https://doi.org/10.1080/15481603.2025.2488595.
128. Irakulis-Loitxate, I.; Gorrono, J.; Zavala-Araiza, D.; Guanter, L. Satellites Detect a Methane Ultra-emission Event from an Offshore Platform in the Gulf of Mexico. *Environ. Sci. Technol. Lett.* **2022**, *9*, 520–525. https://doi.org/10.1021/acs.estlett.2c00225.
129. National Institute for Environmental Studies (NIES). Greenhouse Gases and Water Cycle Observing Satellite (GOSAT-GW) Launch Announcement. 2025. Available online: https://www.env.go.jp/en/press_00032.html (accessed on 2026/04/15).
130. Tanimoto, H.; Matsunaga, T.; Someya, Y.; Fujinawa, T.; Ohyama, H.; Morino, I.; Yashiro, H.; Sugita, T.; Inomata, S.; Müller, A.; et al. The greenhouse gas observation mission with Global Observing SATellite for Greenhouse gases and Water cycle (GOSAT-GW): Objectives, conceptual framework and scientific contributions. *Prog. Earth Planet. Sci.* **2025**, *12*, 8. https://doi.org/10.1186/s40645-025-00684-9.
131. European Space Agency. *First MetOp-SG satellite and Sentinel-5A Launched*; European Space Agency: Paris, France, 2025.
132. GHGsat. *GHGSat Successfully Launches Two New Satellites During COP30*; GHGsat: Montreal, QC, Canada, 2025.
133. The European Space Agency. GHOSt (Global Hyperspectral Observation Satellite). Available online: https://www.eoportal.org/satellite-missions/ghost#missionstatus (accessed on 30 March 2023).
134. Ehret, G.; Bousquet, P.; Pierangelo, C.; Alpers, M.; Millet, B.; Abshire, J.; Bovensmann, H.; Burrows, J.; Chevallier, F.; Ciais, P.; et al. MERLIN: A French-German Space Lidar Mission Dedicated to Atmospheric Methane. *Remote Sens.* **2017**, *9*, 1052. https://doi.org/10.3390/rs9101052.

Disclaimer/Publisher's Note: The statements, opinions and data contained in all publications are solely those of the individual author(s) and contributor(s) and not of MDPI and/or the editor(s). MDPI and/or the editor(s) disclaim responsibility for any injury to people or property resulting from any ideas, methods, instructions or products referred to in the content.